

1 **Cross-reactivity of SARS-CoV structural protein antibodies**
2 **against SARS-CoV-2**

3

4 Timothy A. Bates^{1*}, Jules B. Weinstein^{1*}, Scotland E. Farley^{1*}, Hans C. Leier¹, William B.
5 Messer^{1,2}, Fikadu G. Tafesse^{1#}

6 * These authors contributed equally to this work.

7 # Correspondence should be addressed to F.G.T. (email: tafesse@ohsu.edu)

8

9 ¹ Department of Molecular Microbiology & Immunology, Oregon Health & Science University,
10 Portland, OR 97239, USA

11 ²Department of Medicine, Division of Infectious Diseases, OHSU, Portland, Oregon 97239,
12 USA

13

14

15

16

17

18

19

20

21

22

23

24

25

26

27

28

29

30

31

32

33

34 **Abstract**

35 There is currently a lack of biological tools to study the replication cycle and pathogenesis of
36 SARS-CoV-2, the etiological agent of COVID-19. Repurposing the existing tools, including
37 antibodies of SARS-CoV, is an effective way to accelerate the development of therapeutics for
38 COVID-19. Here, we extensively characterized antibodies of the SARS-CoV structural proteins
39 for their cross-reactivity, experimental utility, and neutralization of SARS-CoV-2. We assessed a
40 total of 10 antibodies (six for Spike, two for Membrane, and one for Nucleocapsid and Envelope
41 viral protein). We evaluated the utility of these antibodies against SARS-CoV-2 in a variety of
42 assays, including immunofluorescence, ELISA, biolayer interferometry, western blots, and
43 micro-neutralization. Remarkably, a high proportion of the antibodies we tested showed cross-
44 reactivity, indicating a potentially generalizable theme of cross-reactivity between SARS-CoV
45 and SARS-CoV-2 antibodies. These antibodies should help facilitate further research into
46 SARS-CoV-2 basic biology. Moreover, our study provides critical information about the
47 propensity of SARS-CoV antibodies to cross-react with SARS-CoV-2 and highlights its
48 relevance in defining the clinical significance of such antibodies to improve testing and guide the
49 development of novel vaccines and therapeutics.

50

51

52

53

54

55

56

57

58

59

60

61

62

63

64

65

66

67

68 Introduction

69 The recent emergence of the novel severe acute respiratory syndrome coronavirus 2 (SARS-
70 CoV-2) in late 2019 has led to an ongoing global COVID-19 pandemic and public health crisis
71 [1]. At the time of writing, there are over seven million confirmed infections and four hundred
72 thousand fatalities globally [2]. SARS-CoV-2 has been designated as a strain of the same
73 species as the original SARS coronavirus (SARS-CoV) due to a high degree of sequence
74 similarity [3]. SARS-CoV-2 falls within the family *Coronaviridae*, and can be further
75 subcategorized as a *Betacoronavirus* of lineage B [3]. There is an urgent need for tools to study
76 this novel coronavirus, as part of the effort to quickly and safely develop vaccines and
77 treatments. One avenue that merits exploration is the repurposing of reagents that were
78 developed for use with SARS-CoV, as many are both extremely effective and commercially
79 available.

80

81 Coronaviruses (CoVs) are enveloped, positive-sense, single-stranded RNA viruses with
82 exceptionally large genomes of up to 32 kb on a single RNA molecule. In the case of SARS-
83 CoV-2, two open reading frames code for sixteen nonstructural proteins and other individual
84 open reading frames are responsible for four structural proteins: spike (S), nucleocapsid (N),
85 membrane (M), and envelope (E) and nine accessory proteins [4]. *Coronaviridae* are a large
86 and diverse family of viruses, with several genera further divided into several lineages, and
87 human and animal coronaviruses are intermixed within each of these categories (Forni et al.,
88 2017[5]. Of the human coronaviruses, the SARS-CoVs are most closely related to the lineage C
89 beta-CoV MERS, followed by the lineage A beta-CoVs HCoV-HKU1 and HCoV-OC43, and then
90 the alpha CoVs HCoV-NL63 and HCoV-229E. The lineage A beta-CoVs and the alpha-CoVs
91 are globally distributed with seroprevalence exceeding 90% in some studies, though they cause
92 relatively mild disease compared to the rarer acute respiratory syndrome coronaviruses [6,7].

93

94 The four SARS-CoV-2 structural proteins are critical for shaping the physical form of the virion,
95 but most available information about them has been extrapolated from other coronaviruses.
96 Generally, the CoV M protein is involved in shaping the viral envelope membrane [8], the N
97 protein complexes with the viral RNA [9], the S protein mediates receptor recognition and
98 membrane fusion [10,11], and the E protein contributes to the structure of the viral envelope
99 [12]. Furthermore, several of these CoV structural proteins have been shown to have
100 intracellular functions unrelated to their role as structural proteins [9]. There are limits to the
101 utility of extrapolation; it is known, for example, that the topology of the CoV envelope protein

102 varies dramatically between various viruses [12], and the differences between the receptor
103 binding domains (RBDs) of the spike protein can be dramatic. Therefore, tools to interrogate the
104 specific functions of each of the SARS-CoV-2 structural proteins would be of immense and
105 immediate use.

106
107 CoV specific antibodies are one type of tool used in such studies. Antibodies against the SARS-
108 CoV-2 structural proteins could be used as reagents in microscopy and western blotting, as
109 structural tools to probe functional epitopes, and even as antiviral therapies. The protein which
110 produces the greatest SARS-CoV-2 specific antibody response in humans is the viral S protein
111 [13], but it is known that antibodies are produced against the N, M, and E proteins as well [7,13].
112 Since SARS-CoV and SARS-CoV-2 are such markedly similar viruses, as discussed below, it is
113 reasonable to assume that there may be some cross-reactivity between SARS-CoV antibodies
114 against their cognate SARS-CoV-2 structural proteins, and, indeed, there is already some
115 evidence that this is the case [14–17].

116
117 SARS-CoV and SARS-CoV-2 S proteins share 76% amino acid sequence homology and both
118 rely on cellular angiotensin-converting enzyme 2 (ACE2) as an attachment receptor as well as
119 the TMPRSS2 protease for priming [18]. Recent reports have identified cross-reactive
120 antibodies that bind to the S protein of both SARS-CoV and SARS-CoV-2, however no such
121 cross-reactive antibodies have been identified for the remaining structural proteins [14–17]. A
122 non-human-primate model of SARS-CoV-2 DNA vaccination found that a polyclonal antibody
123 response to S alone is sufficient to protect from SARS-CoV-2 challenge, similar to results from a
124 human S-only vaccine trial for SARS-CoV [19,20]. Additionally, convalescent plasma from
125 recovered COVID-19 cases has been broadly shown to reduce mortality of individuals with
126 serious disease [21,22]. The sequence similarity between SARS-CoV and CoV-2 N, M, and E
127 proteins are high, at 91%, 90%, and 95% respectively, making it likely that any individual
128 antibody may be cross-reactive. Indeed, there are reports of human antibodies against the S, N,
129 and M proteins for which the epitopes are identical between SARS-CoV and SARS-CoV-2,
130 further supporting the possibility of cross-reactivity, though none have been experimentally
131 verified [13].

132
133 If cross-reactivity with SARS-CoV-2 is a common feature of SARS-CoV antibodies, then many
134 recovered SARS-CoV patients may still possess SARS-CoV-2 reactive antibodies; antibody
135 responses were shown to remain at high levels for at least 12 years according to a recent

136 preprint [23]. While sequence conservation is lower for more common human coronaviruses,
137 their high prevalence may lead to widespread antibodies with cross-reactivity to SARS-CoV-2.
138 Furthermore, antibodies promoting antibody-dependent cellular phagocytosis have been shown
139 to assist in elimination of SARS-CoV infection, showing that cross-reactive antibodies need not
140 be neutralizing to play a productive role in resolution of coronavirus infection [24].

141

142 This report characterizes a series of SARS-CoV monoclonal antibodies for cross-reactivity,
143 experimental utility, and neutralization of the SARS-CoV-2 virus. Information about how
144 antibodies from different coronavirus infections interact is critical for several reasons. It is an
145 important factor to consider during the design of antibody-based coronavirus tests, particularly
146 for those as closely related as SARS-CoV and SARS-CoV-2. New treatments for SARS-CoV-2
147 that interact with a patients immune system will also need to take into account the prevalence of
148 cross-reactive antibodies due to previous coronavirus infections. Further, information about the
149 basic biology of this novel virus will be critical in developing such tailored treatments, and cross-
150 reactive antibodies could be extremely useful in such studies.

151

152

153

154

155

156

157

158

159

160

161

162

163

164

165

166

167

168

169

170 Results

171

172 Sequence similarities of the structural proteins of human coronaviruses

173 The Biodefense and Emerging Infections (BEI) Research Resources Repository has available
174 several types of antibodies and immune sera against each of the structural SARS-CoV proteins
175 as well as whole virus (summarized in Table 1). Eight of these are mouse monoclonal

Antibody	Reference	Protein Specificity	Species	Class	Neutralization of SARS-CoV	Epitope
240C	Tripp et al.	S	Mouse	IgG2a	No	S _A (490-510)
341C	Tripp et al.	S	Mouse	IgG2a	Yes	S _A (490-510)
540C	Tripp et al.	S	Mouse	IgG2a	Yes	S _A (490-510)
154C	Tripp et al.	S	Mouse	IgM	No	S _B (270-350)
CR3022	Ter Meulen et al.	S	Human	IgG1	Yes	S _C (369-519)
NRC-772	Made by BEI	S	Rabbit	serum	Yes	
427C	Tripp et al.	E	Mouse	IgM	No	
19C	Tripp et al.	M	Mouse	IgM	No	
283C	Tripp et al.	M	Mouse	IgG1	No	
42C	Tripp et al.	N	Mouse	IgM	No	

Table 1: SARS-CoV antibodies utilized by this study

176 antibodies of either the IgM, IgG2a, or IgG1 class, recognizing either the SARS-CoV E, M, N, or
177 S proteins. Of these, only two are neutralizing, 341C, and 540C [25]. There are also polyclonal
178 rabbit sera against the SARS-CoV S protein, and an anti-S monoclonal human IgG1 antibody
179 isolated from a SARS-CoV patient [26], all of which are neutralizing.

180 To begin to evaluate structural potential for cross-reactivity, we compared the amino acid
181 sequences of each SARS-CoV-2 structural protein with the homologous protein from the other
182 HCoVs (Figure 1A). We first looked at the amino acid homology among the S proteins of the
183 common human coronaviruses, and found that other human beta-CoVs (MERS-CoV, HCoV-
184 HKU1 and HCoV-OC43) show only about 30% similarity to the SARS-CoV-2 S protein, and
185 human alpha-CoVs (HCoV-229E and HCoV-NL63) show only about 24% similarity to SARS-
186 CoV-2 S protein. The S protein of the original SARS-CoV, however, is much more closely
187 related, showing 77% similarity between SARS-CoV and SARS-CoV-2, which lends support to
188 the idea that anti-SARS-CoV S antibodies could be cross-reactive with the SARS-CoV-2 S
189 protein. The E, M, and N protein sequences show striking similarity between SARS-CoV and
190 SARS-CoV-2; they are 96%, 91%, and 91% similar, respectively (Figure 1A).

191

192 While antibodies that recognize each of the structural proteins are of interest as experimental
193 tools, antibodies that recognize the S protein are particularly so because of their potential to

194 neutralize infectious virus. Structural information about the specific biochemical interactions
 195 between S-specific antibodies and the S protein is of great value. For the anti-S monoclonal
 196 antibodies (through BEI Resources) described in Table 1, the epitopes can be traced to one of
 197 three regions of the RBD. While 240C, 341C, and 540C all bind within a region at the end of the
 198 RBD (epitope S_A) [25], the 154C antibody binds to a region at the beginning of the RBD (epitope
 199 S_B); and the human monoclonal antibody CR3022 binds to specific residues in a broad region in
 200 the middle of the RBD (epitope S_C) [17]. These epitopes are indicated in figure 1B, along with
 201 the alignment of the SARS-CoV and SARS-CoV-2 RBDs. While not identical, these regions do
 202 show some level of similarity between the two virus strains. The three dimensional structure of
 203 the spike protein in both monomeric and the functional trimeric form is displayed to illustrate the
 204 general accessibility of each portion of the protein (Figure 1C).
 205

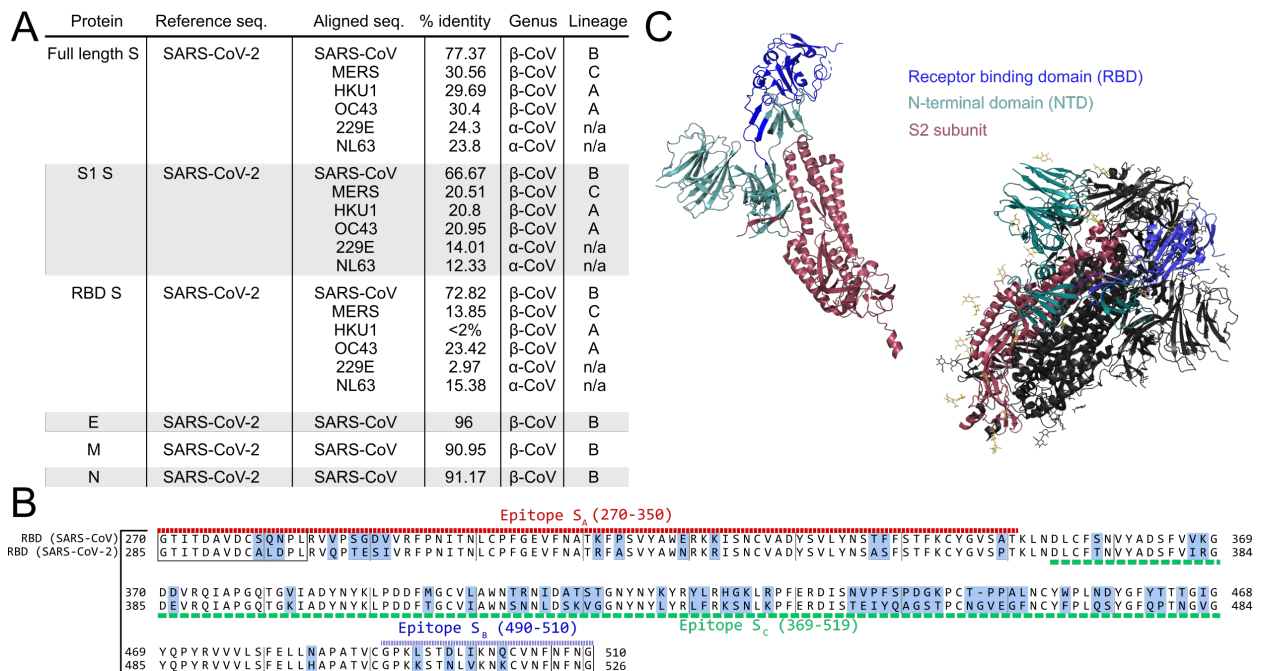


Figure 1: Sequence similarity between SARS-CoV and SARS-CoV-2. (A) Similarity scores for each of the SARS-CoV-2 structural proteins compared with SARS-CoV and other common coronaviruses. Similarity in the S protein is substantially lower than for the other structural proteins. (B) Crystal structure of the S protein color coded by domain both alone and in the functional homotrimeric form where one of the monomers is colored while the other two are in gray. The trimer shows glycosylation sites in yellow. As shown, the NTD and RBD compose the majority of the S1 region. (C) Sequence alignment of the receptor binding domain (RBD) of SARS-CoV and SARS-CoV-2. Regions of difference are highlighted in blue while the epitopes of the antibodies used in this study are underlined according to their designations in Table 1. The boxed regions fall outside of the canonical RBD sequence, but are included due to overlap with the above epitope regions.

207 **Antibodies of the SARS-CoV structural proteins show cross-reactivities with SARS-CoV-**
208 **2 by microscopy**
209

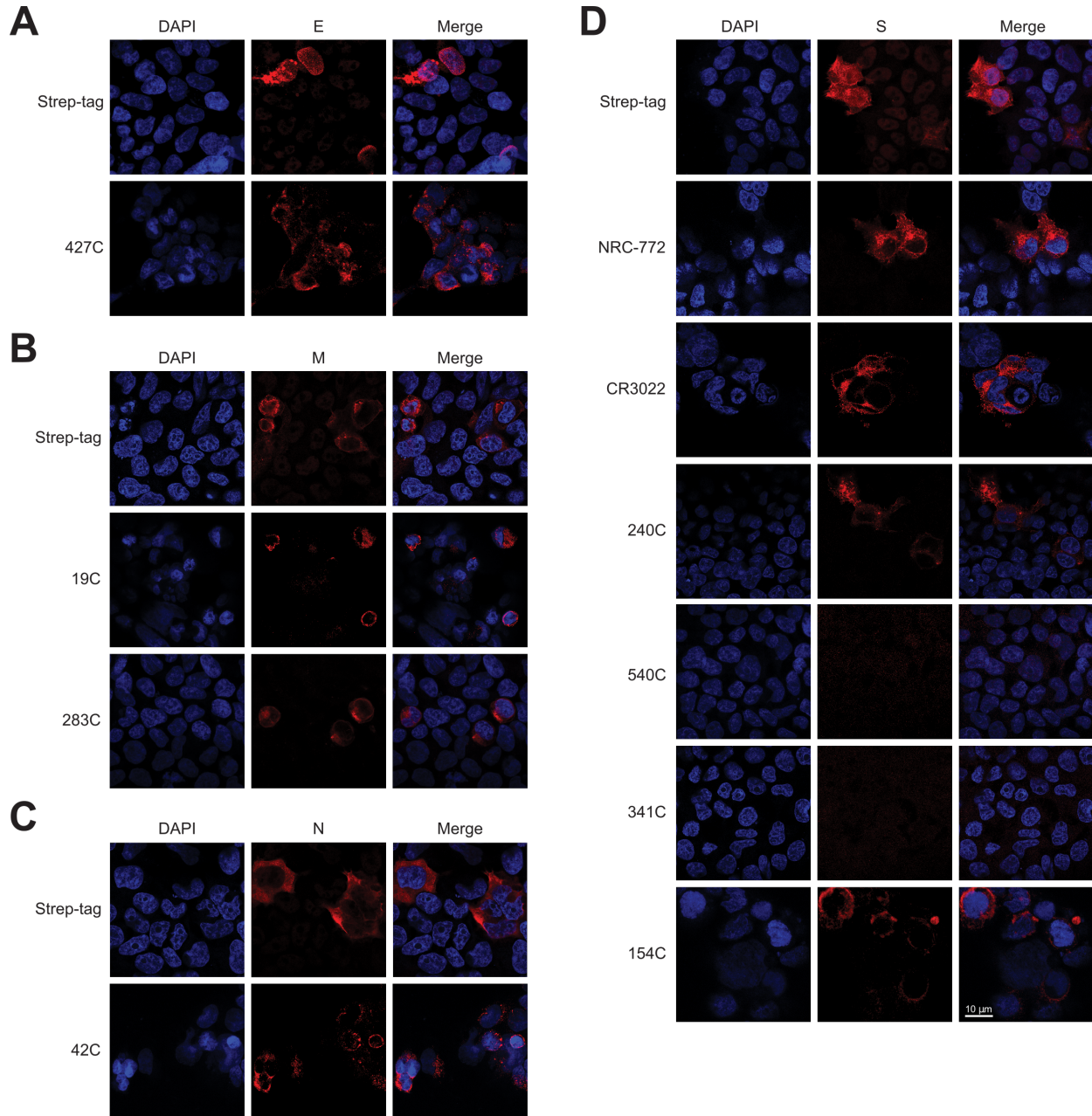


Figure 2: Immunofluorescence of SARS-CoV-2 structural proteins using SARS-CoV antibodies at 63× magnification. Representative immuno-fluorescence images of HEK 293T cells transiently transfected with SARS-CoV-2 structural proteins. 24 h post-transfection, cells were fixed and stained with the listed SARS-CoV antibodies: (A) Envelope, (B) Membrane, (C) Nucleocapsid, and (D) Spike proteins. All proteins are strep-tagged and control stained with anti-strep-tag antibody or the indicated antigen-specific antibody (Red). DAPI (Blue) was used to visualize cell nuclei.

211 To assess SARS-CoV antibodies against SARS-CoV-2, we first performed
 212 Immunofluorescence(IF) staining of 293T cells transiently transfected with Strep-tagged
 213 constructs of each of the individual SARS-CoV-2 structural proteins [27]. We compared the
 214 staining of the Strep-tag within each structural protein in immunofluorescence against that of the
 215 experimental antibodies, finding that the staining pattern of a majority of these antibodies as
 216 detectable, with some being highly similar to the strep-tag antibody (Figure 2 and S2). The E, M,
 217 and S proteins each had at least one high-quality antibody while the only N-specific antibody did
 218 not perform well, as was reported for these antibodies against SARS-CoV [25]. Together, these
 219 antibodies provide nearly complete coverage of SARS-CoV-2 structural proteins, showing their
 220 utility for SARS-CoV-2 experiments involving microscopy.

221

222 **Antibodies of the SARS-CoV structural proteins show cross-reactivities with SARS-CoV-**
 223 **2 by immunoblotting**

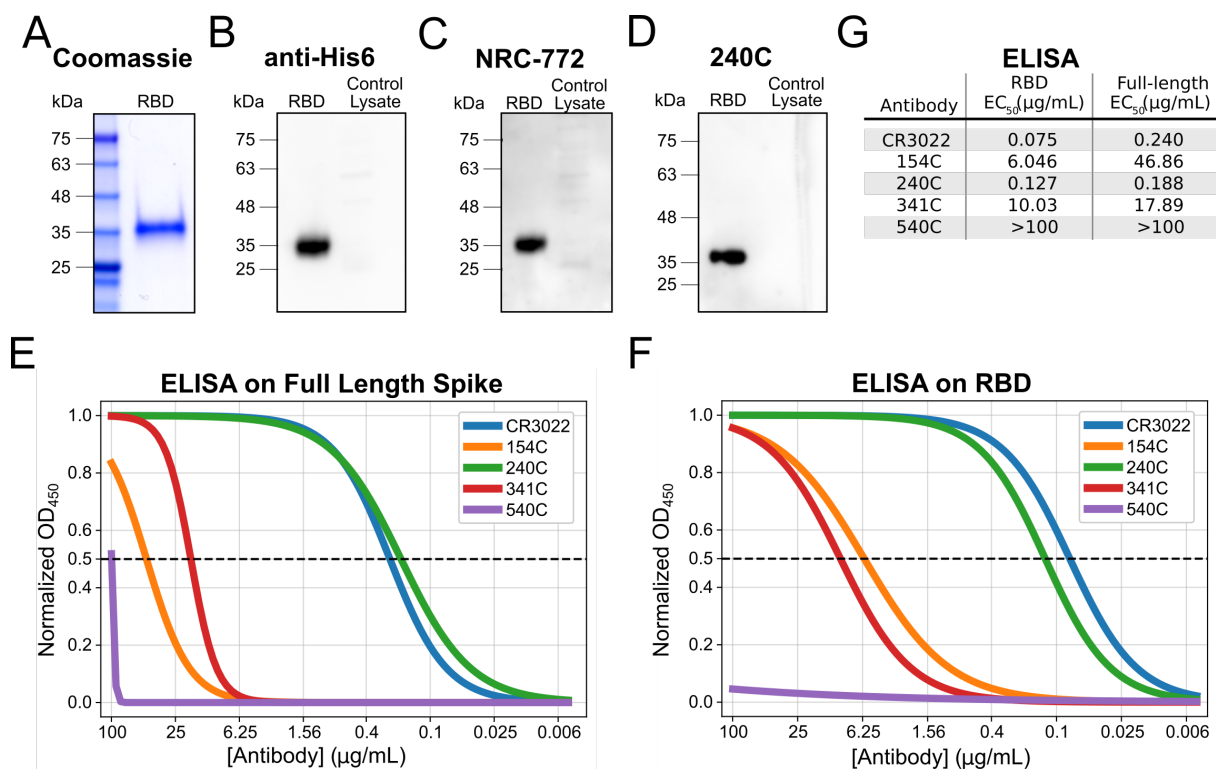


Figure 3: Biochemical characterization of Spike protein specific antibodies. Characterization of the S-specific antibodies by western blot and ELISA. (A) Coomassie stain of in-house purified His6-tagged RBD protein produced in HEK 293-F suspension cells and purified by Ni-NTA chromatography. (B-D) Western blot of purified RBD protein probed with control α -His6 or 240C. 1 μ g purified RBD was loaded for each blot and untransfected HEK 293T control lysate was included to monitor non-specific binding. The 240C antibody was the only antibody to demonstrate binding in western blots (see Supplementary Figure 2 for details). (E) ELISA on purified full length Spike coated at 2 μ g/mL. (F) ELISA on purified RBD coated at 2 μ g/mL. (G) Summary table of observed EC₅₀ values from both sets of ELISAs.

224

225 We next evaluated these antibodies in western blotting. His₆-tagged RBD from SARS-CoV-2
226 was produced in HEK 293 cells and purified by Ni-NTA chromatography (Figure 3A). This RBD
227 was then used for a western blot with each of the mouse monoclonal antibodies (Figure 3B-D).
228 The staining produced by each experimental antibody was compared to anti-His₆ staining of the
229 RBD as a positive control, and lysate from untransfected 293T cells to assess background. Of
230 these antibodies, 240C and NR-772 produced strong signal with little background, whereas the
231 other monoclonal antibodies did not produce detectable signal (Figure S3).

232

233 **Spike antibodies show cross-reactivity in binding**

234

235 The fact that the S glycoprotein is responsible for virus binding and entry into host cells makes it
236 an attractive target for antibody generation as some of these antibodies may be neutralizing.
237 Because of the potential functional role for these antibodies, and because of the number of
238 different antibody clones, we decided to examine the S-protein-specific antibodies more
239 thoroughly.

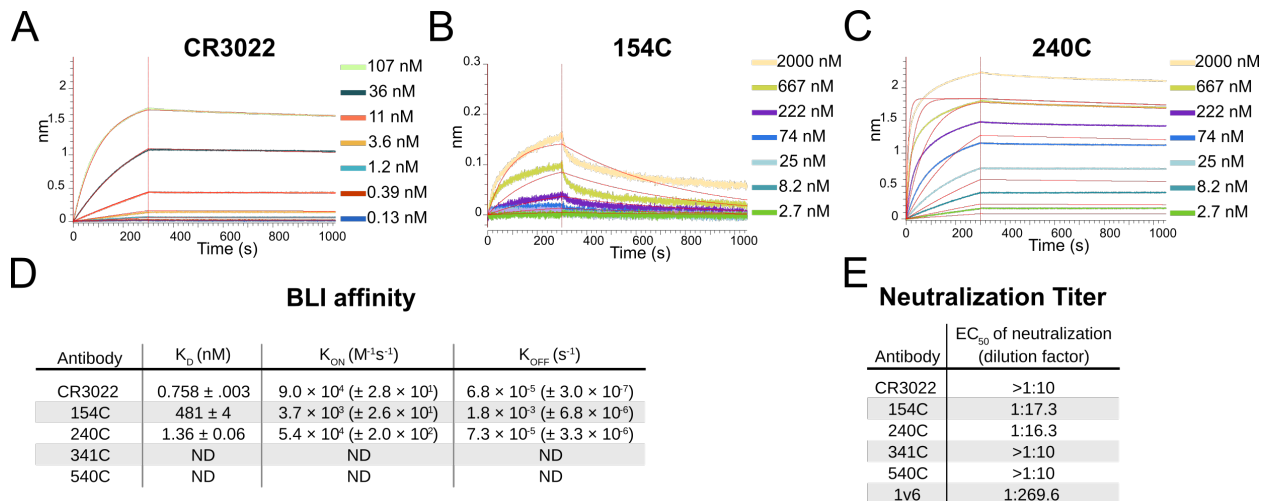
240

241 We assessed the binding of the S-protein-specific antibodies to both the full-length SARS-CoV-
242 2 S protein and the purified Receptor Binding Domain (RBD) by ELISA (Figure 3E-F and Figure
243 S4, summarized in Figure 3G). CR3022 and 240C showed strong binding to both the full-length
244 spike and the RBD (EC₅₀ 75 ng/mL and 127 ng/mL, respectively, to the RBD). 154C and 341C
245 showed weak but detectable binding (6.046 µg/mL and 10.03 µg/mL, respectively, to the RBD),
246 while 540C did not demonstrate binding at all. The trend for these antibodies is generally similar
247 to what was seen in the previous studies where the antibodies were tested against recombinant
248 SARS-CoV S protein [25]. The original report of CR3022 did not perform a direct ELISA for us to
249 compare our results to, however our data agree with studies of CR3022 on SARS-CoV-2
250 showing that it binds strongly to both full-length spike and the RBD [17]. While CR3022 appears
251 to be the strongest binder to RBD, 240C is marginally better on the full-length spike protein.

252

253 To assess the binding kinetics of the antibody-RBD interaction in more detail, we measured the
254 antibody-epitope interactions using biolayer interferometry (BLI). The three monoclonal
255 antibodies that showed strongest-binding with the ELISA displayed high affinity for the SARS-
256 CoV-2 RBD, CR3022 showed the strongest binding with a calculated K_D of 758 pM (Figure 4A),
257 while 240C demonstrated a 1.36 nM K_D (Figure 4B), and 154C a 481 nM K_D (Figure 4C). As

258 summarized in figure 4D, these antibodies showed fast-on/slow-off kinetics in agreement with a
 259 previous report of CR3022 binding kinetics on RBD [17]. The other antibodies we tested
 260 displayed no measurable binding at the highest concentration used (Figure S5). Importantly, BLI
 261 does not account for the avidity of these antibodies, and it is likely that the interaction of each
 262 epitope/paratope pair is substantially lower than that of the intact antibody; however, the intact
 263 antibody more closely resembles the interaction that is likely to occur in most *in vitro* assays, or
 264 indeed *in vivo*. Our K_D is substantially lower than reported in Tian et al., however this is likely
 265 due to differences in the reagents used [15]. Tian et al. expressed their RBD in *E. coli*,
 266 preventing glycosylation, while our RBD was produced in mammalian cells. Additionally, their
 267 CR3022 was produced as a single chain variable fragment (scFv) in *E. coli*, which would contain
 268 only a single paratope and may fold differently than our full CR3022 antibody, which was
 269 produced in a plant expression system.



270 Figure 1: Binding Kinetics and functional testing of Spike specific antibodies against the RBD of the
 271 SARS-CoV-2. (A-C) Bi-layer interferometry curves for CR3022, 154C, and 240C with three-fold dilutions.
 Streptavidin biosensors were coated with biotinylated RBD, then blocked with 1 μ M D-Biotin in kinetics
 buffer. Negative binding curves for 341C and 540C shown in figure S4. Curve fitting was performed
 using 1:1 binding model in ForteBio Analysis HT 10.0 software. (D) Summary of quantified binding
 kinetics of Spike monoclonal antibodies from BLI experiment. (E) Neutralization assay 50% neutralization
 values against SARS-CoV-2 Spike pseudotyped lentivirus. 1v6 is positive control from COVID-19 patient
 convalescent serum collected at day 14. The concentration of all monoclonal antibody stocks was 1 mg/
 mL. 154C and 240C showed only partial neutralization at the highest concentration tested (1:10 dilution),
 while 341C, 540C, and CR3022 failed to reliably neutralize pseudotyped virus at this dilution.

272 Spike antibodies of SARS-CoV show limited cross-neutralization of SARS-CoV-2

273
 274 Finally, we assessed the neutralizing capabilities of these S protein-specific monoclonal
 275 antibodies. We set up a neutralization assay using a Lentivirus GFP-reporter pseudotyped with

276 the SARS-CoV-2 S protein [28]. Neutralization was assessed by microscopy, using the area of
 277 GFP expression compared to that of an antibody-untreated control. Serial dilutions of antibodies
 278 were used to generate neutralization curves and estimate the antibody concentration necessary
 279 for 50% neutralization. This readout was used because the monoclonal antibodies displayed
 280 only partial neutralization at the highest concentration used in our assay. To validate our assay,
 281 we used human convalescent serum from a SARS-CoV-2 positive patient. This anti-serum
 282 demonstrated 50% neutralization at a dilution of 1:270 (Figure 4E). Consistent with a previous
 283 report, CR3022 failed to show any neutralization at 100 µg/mL despite its potent binding in
 284 every other assay [17]. 154C and 240C both showed partial neutralization, with a 50% reduction
 285 in GFP area at 57.8 µg/mL and 61.3 µg/mL respectively. Consistent with the BLI results, 341C
 286 and 540C did not show substantial neutralization. We were surprised to see 154C perform the
 287 best in this assay, particularly because the original report of these antibodies on SARS-CoV
 288 showed 341 and 540 as the only antibodies with neutralizing capabilities. One unique aspect of
 289 154C is that it is the only IgM antibody from this selection of Spike-specific antibodies, however
 290 it is not clear how this might affect neutralization.

291

292 **Summary of cross-reactivity of SARS-CoV structural-protein-specific antibodies to**
 293 **SARS-CoV-2 structural proteins in various assays**

Summary of reagent quality in assays

Antibody	Protein target	Immunofluorescence	ELISA	Western blot	Biolayer interferometry	Neutralization
240C	S	+++	+++	+++	+++	partial
154C	S	+	++	-	+	partial
341C	S	+	++	-	-	-
540C	S	-	-	-	-	-
CR3022	S	++	+++	-	+++	-
NRC-722	S	+++	ND	+++	+++	ND
42C	N	-	ND	-	ND	ND
427C	E	++	ND	-	ND	ND
19C	M	+	ND	-	ND	ND
283C	M	+++	ND	-	ND	ND

Table 2: Summary of antibody quality for different assays. Qualitative utility scores (+++) very good, (++) good, (+) moderate, (-) fail were assigned to each antibody for each assay in which it was tested; (partial) indicates incomplete neutralization at 100 µg/mL and (ND) indicates that an antibody was not used in this particular assay.

294 The utility of each of the antibodies used in this study has been summarized in Table 2. In
 295 particular, the S-protein-specific 240C performed well in every assay we performed, excluding
 296 neutralization. In contrast, 540C showed no detectable binding in any of our assays. The other
 297 S-protein-specific monoclonal antibodies 154C, 341C, and CR3022 showed mixed utility in
 298 different assays. The rabbit polyclonal antibody NRC-772 also worked in every assay in which it

299 was tested, however, polyclonal sera is limited to experiments where structural information
300 about particular epitopes is not important due to the unknown admixture of the contained
301 antibody clones. The antibodies against E, M, and N demonstrated utility in
302 immunofluorescence, but not western blot. Further studies could explore these antibodies in
303 greater detail by producing purified E, M, and N proteins for use in biochemical assays such as
304 the ones we used to characterize the S-protein-specific antibodies in this report.

305

306

307

308

309

310

311

312

313

314

315

316

317

318

319

320

321

322

323

324

325

326

327

328

329

330

331

332

333 Discussion

334

335 Our results demonstrate substantial cross-reactivity from a majority of the SARS-CoV-2
336 structural-protein-targeted antibodies that we evaluated. This is the first report of cross-reactive
337 antibodies directed against the N, M, and E proteins. These tools can be readily obtained from
338 BEI resources and utilized by labs to study the properties of untagged SARS-CoV-2 structural
339 proteins. These antibodies can serve the unmet need for more resources enabling the study of
340 the SARS-CoV-2. It is critical to understand the basic biology of SARS-CoV-2 in order to inform
341 efforts towards improved diagnostics and treatments. Further, information about cross-reactivity
342 of antibodies between SARS-CoV and SARS-CoV-2 may assist bioinformatics labs in
343 developing computational tools for predicting cross-reactivity of other antibodies, or even
344 guiding rational design of improved coronavirus antibodies and small-molecule therapeutics.

345

346 We have shown that these publicly available antibodies are of potential use in several different
347 types of assays with SARS-CoV-2 proteins. We found that several of these SARS-CoV-2
348 structural protein antibodies demonstrated good staining in immunofluorescence (240C, NRC-
349 772, and CR3022 against S; 283C against M; 427C against E). The anti-S antibodies, 240C and
350 NRC-772, also give clear signal in western blot with minimal background. Several S antibodies
351 show potent binding to full-length S and the RBD by ELISA, as well as binding to the RBD by
352 biolayer interferometry (240C, CR3022, and NRC-772). This wide range of uses substantially
353 broadens our ability to investigate the biochemical properties of SARS-CoV-2 structural
354 proteins.

355

356 Although these antibodies only partially neutralized a SARS-CoV-2 model infection, they are still
357 of interest for their potential to elucidate the structure and function of their protein targets.
358 Antibodies have been critical tools in structure determination and in the mapping of proteins'
359 functional regions. Having a wide array of antibodies that recognize varying epitopes is of great
360 help in this endeavor. Additionally, with the current dearth of knowledge regarding the life cycle
361 and pathogenesis of SARS-CoV-2, particularly regarding the understudied M, N, and E proteins,
362 we believe that these antibodies could be used in experiments to better understand the nuances
363 of their functions beyond their obvious structural roles.

364

365 Our results also speak to the high proportion of SARS-CoV antibodies that display substantial
366 cross-reactivity to SARS-CoV-2 structural proteins. Anecdotal evidence supports the efficacy of

367 convalescent plasma treatment for COVID-19, indicating that cross-reactive antibodies
368 generated during previous coronavirus infections may prove beneficial during coronavirus
369 infection [29]. Conversely, studies of COVID-19 patients have found neutralizing antibody titers
370 to be directly proportional to disease severity, suggesting a more complicated relationship
371 between antibodies and COVID-19 [30,31]. Some have hypothesized that this may be due to
372 high concentrations of virus and neutralizing antibodies acting together to drive greater immune
373 pathology [32,33]. A better understanding of the functions of individual antibody isotypes
374 against different antigenic targets will be critical to predicting the utility of a particular antibody
375 against SARS-CoV-2.

376
377 Further studies could also investigate possible cooperation between antibodies recognizing
378 different epitopes, especially as CR3022 neutralization was shown to have synergy with another
379 anti-S antibody which recognized a different epitope on the protein [26]. A recent study [34], for
380 example, characterized a neutralizing monoclonal antibody that did not bind the RBD at all, and
381 instead recognized an epitope in the NTD of the S protein. Knowledge about the variety of
382 vulnerable epitopes, and possible synergy between antibodies that target them, brings us ever
383 closer to being able to design and deploy effective therapeutics and vaccines in this time of
384 urgent need.

385

386

387

388

389

390

391

392

393

394

395

396

397

398

399

400

401 **STAR★ Methods**

402

Reagent or Resource	Identifiers	Source
Antibody		
Human monoclonal anti-SARS-CoV -S Cr3022	NR-52392	BEI Resources
Mouse anti-SARS-CoV S Monoclonal IgM 154c	NR-620	BEI Resources
Mouse anti-SARS-CoV S Monoclonal IgG2a 240c	NR-616	BEI Resources
Mouse anti-SARS-CoV S Monoclonal IgG2a 341c	NR-617	BEI Resources
Mouse anti-SARS-CoV S Monoclonal IgG2a 540c	NR-618	BEI Resources
Mouse anti-SARS-CoV M Monoclonal IgM 19c	NR-615	BEI Resources
Mouse anti-SARS-CoV M Monoclonal IgG1 283c	NR-621	BEI Resources
Mouse anti-SARS-CoV E Monoclonal IgM 472c	NR-614	BEI Resources
Mouse anti-SARS-CoV N Monoclonal IgM 42c	NR-619	BEI Resources
Rabbit anti-SARS-CoV S polyclonal sera-hydrogel	NRC-773	BEI Resources
Rabbit anti-SARS-CoV S polyclonal sera	NRC-768	BEI Resources
Guinea pig anti-SARS-CoV S polyclonal sera	NR-10316	BEI Resources
Mouse anti-2xStrep monoclonal	SAB2702215	Sigma Aldrich

antibody		
Goat anti-mouse HRP IgG	HAF007	R & D Systems
Goat anti-mouse HRP IgM	62-6820	Invitrogen
Donkey anti-human HRP	SAB3701359	Sigma Aldrich
antiHis-HRP	ma1-80218	Invitrogen
anti-Human-AlexaFluor488	A11013	Invitrogen
anti-Mouse IgG AlexaFluor555	A21422	Invitrogen
anti-Mouse IgM AlexaFluor488	A21042	Invitrogen
anti-Rabbit FAB2 AlexaFluor555	4413S	Invitrogen
Biological samples		
Human deidentified Patient Sera 1v6	N/A	Messer Lab, OHSU MMI
Human deidentified Patient Sera 0v1	N/A	Messer Lab, OHSU MMI
Chemicals and recombinant proteins		
RBD recombinant purified Sars-CoV-2 Spike	NR-52306	BEI Resources
Full-length Soluble SARS-CoV-2 Spike	NR-52308	BEI Resources
BSA		Gold-Bio
FBS	97068-085	VWR
PBS	17-516F	Lonza Biosciences
Trypsin	25200056	Thermo Fisher Scientific
Recombinant spike protein (His tag), SARS-CoV-2	NR-52309	BEI Resources
Cell line		
HEK 293T	CRL-3216	ATCC
HEK 293T human Ace2	NR-52511	Crawford et al. 2020 ,

expressing stable cell line		Bloom lab, BEI Resources
Recombinant DNA		
HDM_IDTSpike_fixK, SARS-CoV-2 plasmid	NR-52514	Crawford et al. 2020 , Bloom lab, BEI Resources
HDM_Hgpm2	NR-52517	Crawford et al. 2020 , Bloom lab, BEI Resources
HDM_tat1b	NR-52518	Crawford et al. 2020 , Bloom lab, BEI Resources
pRC_CMV_Rev1b	NR-52519	Crawford et al. 2020 , Bloom lab, BEI Resources
pHAGE2_CMV_ZsGreen_W	NR-52520	Crawford et al. 2020 , Bloom lab, BEI Resources
pTwist-EF1alpha-nCoV-2019-S-2xStrep		Gordon et al. 2020 Krogon Lab
pLVX-EF1alpha-nCoV-2019-E-IRES-Puro		Gordon et al. 2020 Krogon Lab
pLVX-EF1alpha-nCoV-2019-M-IRES-Puro		Gordon et al. 2020 Krogon Lab
pLVX-EF1alpha-nCoV-2019-N-IRES-Puro		Gordon et al. 2020 Krogon Lab
Plasmid pCAGGS, Spike protein(soluble),SARS-CoV-2,w/his tag	NR-52309	BEI Resources
Plasmid pcDNA3.1 SARS-CoV-2 Spike ectodomain (His)	NR-52421	BEI Resources
Plasmid pMCSG53 SARS-CoV-2, Spike RBD (His)	NR-52430	BEI Resources

Software		
R	N/A	rstudio.com
Python	N/A	python.org
Critical Commercial Assays		
PureLink™ HiPure Plasmid Maxiprep Kit	K210007	Invitrogen
ChromaLINK biotin protein labeling kit	B-9007-105K	Vector Labs
Streptavidin (SA) Biosensors	18-5019	ForteBio
Other		
NuncSorp ELISA Plates		Thermo Fisher Scientific
Nitrocellulose membrane		

403

404 **Resource Availability**

405

406 **Lead contact**

407

408 Further information and requests for resources and reagents should be directed to and
409 will be fulfilled by the Lead Contact, Fikadu Tafesse (tafesse@ohsu.edu).

410

411 **Materials availability**

412

413 No unique reagents were generated during the course of this study.

414

415 **Data and software availability**

416

417 This study did not generate any unique datasets or code.

418

419 **Experimental Model and Subject Details**

420

421 293T stable cell lines expressing Ace2 receptor (293T-Ace2) were a kind gift from Dr.
422 Jesse D. Bloom from University of Washington, and described previously (Crawford et
423 al. 2020). Wt low-passage 293T cells (293T-Lp) and 293T-Ace2 were cultured in
424 Dulbecco's Modified Eagle Medium (DMEM, 10% FBS, 1% Penn-Strep, 1% NEAA) at
425 37C. Cells were cultured on treated T75 dishes, passaged with Trypsin at 95%
426 confluency to avoid overcrowding.

427

428 **Method Details**

429

430 **Sequence alignment**

431 Protein sequences were obtained from uniprot and aligned using the T-Coffee multiple
432 sequence alignment server.

433

434 **Cell transfection**

435 Transfections were carried out in 293T cells seeded at 70-90% cell density using
436 Lipofectamine 3000 (ThermoFisher Scientific) as per manufacturer's instructions. For
437 immunofluorescence, the SARS-CoV2 structural protein plasmids pTwist-EF1alpha-
438 nCoV-2019-S-2xStrep, pLVX-EF1alpha-nCoV-2019-E-IRES-Puro, pLVX-EF1alpha-
439 nCoV-2019-M-IRES-Puro, or pLVX-EF1alpha-nCoV-2019-N-IRES-Puro were
440 transfected using 2µg of plasmid per well of a 24-well plate. Structural SARS-CoV-2
441 protein plasmids were a kind gift from the Krogan Lab at UCSF and are described
442 previously (Gordon et al 2020). For pseudotyped lentivirus production, lentivirus
443 packaging plasmids, HDM_Hgpm2, HDM_tat1b, PRC_CMV_Rev1b, SARS_CoV-2 S
444 plasmid HDM_IDTSpike_fixK, and LzGreen reporter plasmid
445 pHAGE2_CMV_ZsGreen_W were transfected using 0.44µg for packaging, 0.68µg for S,
446 and 2µg for reporter plasmids per 6 cm dish. Packaging, SARS-CoV-2 S, and reporter
447 plasmids were a kind gift from Jesse D. Bloom from University of Washington, and are

448 described previously (Crawford et al 2020). Transfection media was carefully removed 6
449 hours post transfection, and replaced with DMEM.

450

451 **Pseudotyped lentivirus production**

452 293T cells were seeded at 2 million cells/dish in 6cm TC-treated dishes. The following
453 day, cells were transfected as described above with lentivirus packaging plasmids,
454 SARS-CoV-2 S plasmid, and IzGreen reporter plasmid (Crawford et al., 2020). After
455 transfection, cells were incubated at 37C for 60 hours. Viral media was harvested,
456 filtered with 0.45µm filter, then frozen before use. Virus transduction capability was then
457 tittered on 293T-Ace2 cells treated with 50µl of 5µg/ml polybrene (Sigma-Aldrich LLC).
458 IzGreen titer was determined by fluorescence using BZ-X700 all-in-one fluorescent
459 microscope (Keyence), a 1:16 dilution was decided as optimal for following
460 neutralization assays due to broad transduced foci distribution.

461

462 **Immunofluorescence**

463 293T cells were seeded on 24-well plates containing glass coverslips coated with poly-
464 lysine solution; 100,000 cells were seeded per well. Cells were transfected with SARS-
465 CoV-2 structural protein plasmids as described above. After 48 hours post transfection,
466 cells were fixed with 4% PFA in PBS. Cover slips were permeabilized with 2% BSA,
467 0.1% Triton-X-100 in PBS. Transfected cells were incubated for 3 hours at RT with the
468 following anti-SARS-CoV structural protein monoclonal or polyclonal antibodies at a
469 1:250 dilution: mouse anti-SARS-CoV S monoclonal IgM 154c, mouse anti-SARS-CoV
470 S monoclonal IgG2a 240c, mouse anti-SARS-CoV S monoclonal IgG2a 341c, mouse
471 anti-SARS-CoV S monoclonal IgG2a 540c, mouse anti-SARS-CoV N monoclonal IgM
472 19c, mouse anti-SARS-CoV M monoclonal IgG1 283c, mouse anti-SARS-CoV E
473 monoclonal IgM 472c, mouse anti-SARS-CoV N monoclonal IgN 42c, rabbit anti-SARS-
474 CoV S polyclonal sera (BEI Resources) and mouse anti-2xStrep-tag antibody (Sigma-
475 Aldrich). Anti-mouse IgG AF555, anti-rabbit IgG AF555, or anti-mouse IgM AF488
476 conjugated secondary antibodies were added at 1:500 dilution for 1 hour at RT
477 (Invitrogen). Confocal imaging was performed with a Zeiss LSM 980 using a 63x Plan-
478 Achromatic 1.4 NA oil immersion objective. Images were processed with Zeiss Zen Blue

479 software. Maximum intensity z-projections were prepared in Fiji. All antibody stain
480 images were pseudocolored red for visual consistency.

481

482

483 **Neutralization assay**

484 Neutralization protocol was based on previously reported neutralization research
485 utilizing SARS-CoV-2 S pseudotyped lentivirus (Crawford et al., 2020). 293T-Ace2 cells
486 were seeded on tissue culture treated, poly-lysine treated 96-well plates at a density of
487 10,000 cells per well. Cells were allowed to grow overnight at 37°C. LzGreen SARS-
488 COV-2 S pseudotyped lentivirus were mixed with 2-fold dilutions of the following
489 monoclonal or polyclonal anti-SARS-CoV-2 S antibodies: mouse anti-SARS-CoV S
490 monoclonal IgM 154c, mouse anti-SARS-CoV S monoclonal IgG2a 240c, mouse anti-
491 SARS-CoV S monoclonal IgG2a 341c, mouse anti-SARS-CoV S monoclonal IgG2a
492 540c, rabbit anti-SARS-CoV S polyclonal sera, Guinea pig anti-SARS-CoV S polyclonal
493 sera, human monoclonal anti-SARS-CoV S Cr3022 (BEI Resources). Human patient
494 sera from a SARS-CoV-2 patient was used as positive neutralization control, while virus
495 alone was used as negative control. Sera and antibody dilutions ranged from 1:10 to
496 1:1048. Virus-antibody mixture was incubated at 37C for 1 hour after which virus was
497 added to 293T-Ace2 treated with 5µg/ml polybrene. Cells were incubated with
498 neutralized virus for 44 hours before imaging. Cells were fixed with 4% PFA for 1 hour
499 at RT, incubated with DAPI for 10 minutes at RT, and imaged with BZ-X700 all-in-one
500 fluorescent microscope (Keyence). Estimated area of DAPI and GFP fluorescent pixels
501 was calculated with built in BZ-X software (Keyence).

502

503 **Enzyme-linked immunosorbent assay (ELISA)**

504 ELISA plates, Nunc MaxiSorp (Invitrogen), were coated with purified recombinant
505 SARS-COV2 RBD domain (BIR resources, NR-52306) at 2µg/ul in PBS. Coating was
506 carried out overnight at 4°C. Protein was blocked in 2% BSA, 1% tween-20 in PBS for
507 30 minutes at RT. The following anti SARS-CoV-2 S monoclonal and polyclonal
508 antibodies were serially diluted by 2-fold dilutions in blocking buffer: mouse anti-SARS-
509 CoV S monoclonal IgM 154c, mouse anti-SARS-CoV S monoclonal IgG2a 240c, mouse

510 anti-SARS-CoV S monoclonal IgG2a 341c, mouse anti-SARS-CoV S monoclonal IgG2a
511 540c, human monoclonal anti-SARS-CoV-S Cr3022 (BEI Resources). Human patient
512 sera from a SARS-CoV-2 patient was used as a positive control. Dilutions ranged
513 from 1:10 to 1:10480, and were incubated for 1 hour at RT. Anti-mouse HRP, and anti-
514 human-HRP secondary antibodies were used at 1:4000 concentration in blocking buffer,
515 and were incubated 1 hour at RT. 50 μ L of TMB HRP substrate (ThermoFisher
516 Scientific) was added, and following incubation for 10 minutes at RT, 50 μ L of 2N
517 H₂SO₄ was added as a stopping solution. Plate absorbance at 405nm was measured
518 using a CLARIOstar® Plus plate fluorimeter (BMG Labtech).

519

520 **RBD protein purification and biotinylation**

521 Purified SARS-CoV-2 S-RBD protein was prepared as described previously (Stadlbauer
522 et al., 2020). Briefly, His-tagged RBD bearing lentivirus was produced in HEK 293T cells
523 and used to infect HEK 293-F suspension cells. The suspension cells were allowed to
524 grow for 3 days with shaking at 37°C at 8% CO₂. Cell supernatant was collected, sterile
525 filtered, and purified by Ni-NTA chromatography. The purified protein was then buffer
526 exchanged into PBS and concentrated. For use in BLI, purified RBD was biotinylated
527 using the ChromaLINK biotin protein labeling kit according to the manufacturer's
528 instructions with 5x molar equivalents of labeling reagent to achieve 1.92 biotins/protein.

529

530 **Biolayer interferometry (BLI)**

531 Streptavidin biosensors (ForteBio) were soaked in PBS for at least 30 minutes prior to
532 starting the experiment. Biosensors were prepared with the following steps: equilibration
533 in kinetics buffer (10 mM HEPES, 150 mM NaCl, 3mM EDTA, 0.005% Tween-20, 0.1%
534 BSA, pH 7.5) for 300 seconds, loading of biotinylated RBD protein (10 μ g/mL) in kinetics
535 buffer for 200 seconds, and blocking in 1 μ M D-Biotin in kinetics buffer for 50 seconds.
536 Binding was measured for seven 3-fold serial dilutions of each monoclonal antibody
537 using the following cycle sequence: baseline for 300 seconds in kinetics buffer,
538 association for 300 seconds with antibody diluted in kinetics buffer, dissociation for 750
539 seconds in kinetics buffer, and regeneration by 3 cycles of 20 seconds in 10 mM glycine
540 pH 1.7, then 20 seconds in kinetics buffer. All antibodies were run against an isotype

541 control antibody at the same concentration. Data analysis was performed using the
542 ForteBio data analysis HT 10.0 software. Curves were reference subtracted using the
543 isotype control and each cycle was aligned according to its baseline step. KDs were
544 calculated using a 1:1 binding model using global fitting of association and dissociation
545 of all antibody concentrations, excluding dilutions with response below 0.005 nm.

546

547 **Western blot**

548 293T cells were seeded in 10 cm dishes at a density of 3.5 million cells per dish. After
549 overnight growth, cells were transfected using lipofectamine 3000 as described above.
550 Plasmids pTwist-EF1alpha-nCoV-2019-S-2xStrep, pLVX-EF1alpha-nCoV-2019-E-
551 IRES-Puro, pLVX-EF1alpha-nCoV-2019-M-IRES-Puro, or pLVX-EF1alpha-nCoV-2019-
552 N-IRES-Puro were transfected using 90 µg of DNA per 10 cm dish. Cells were scraped
553 48 hours post-transfection, then lysed in RIPA buffer (EMD Millipore). Cell lysates were
554 diluted with reducing Laemmli buffer, incubated for 10 minutes at 37°C, then ran on 4–
555 20% Mini-PROTEAN® TGX™ Precast Protein Gels (BIO-RAD). Additionally, 1ug of
556 purified recombinant S RBD-His₆ was diluted in PBS and Laemmli buffer to a final
557 volume of 20 µl and added to a 7.5% Mini-PROTEAN® TGX™ Precast Protein Gel (BIO-
558 RAD). Resolved proteins were then transferred to a PVDF membrane, blocked in TBS
559 with 2% BSA 0.1% Tween-20, then incubated with the following antibodies diluted to
560 1:500 in blocking buffer: mouse anti-SARS-CoV N monoclonal IgM 19c, mouse anti-
561 SARS-CoV M monoclonal IgG1 283c, mouse anti-SARS-CoV E monoclonal IgM 472c,
562 and mouse anti-2xStrep-tag antibody, and anti-His-HRP. Blots were stained with
563 SuperSignal™ West Pico PLUS Chemiluminescent Substrate (ThermoFisher Scientific)
564 using an ImageQuant LAS 4000 imager (GE Life Sciences).

565

566 **Quantification and Statistical Analysis**

567

568 The EC₅₀ values were calculated using a three parameter logistic regression model in
569 the Python software package.

570

571 **Acknowledgments**

572

573 This work was supported by NIH training grant T32AI747225 on Interactions at the
574 Microbe-Host Interface and OHSU Innovative IDEA grant 1018784. BLI data was
575 generated on an Octet Red 384, which is made available and supported by the OHSU
576 Proteomics Shared Resource facility and equipment grant number S10OD023413. We
577 acknowledge the support of the members of the Messer lab who performed collection of
578 patient samples, and the patients who agreed to donate samples for scientific research.

579

580 **Author Contributions**

581

582 T.A.B., J.W., and F.G.T. conceived and designed the study. T.A.B., J.W., and H.L.
583 performed the experiments and collected the data. T.A.B. performed data analysis and
584 visualization. T.A.B., S.F., and J.W. wrote the paper, and all authors reviewed and
585 edited the paper.

586

587

588

589

590

591

592

593

594

595

596

597

598

599

600

601

602 **References**

603

604 Ahmed, S.F., Quadeer, A.A., McKay, M.R., 2020. Preliminary Identification of Potential
605 Vaccine Targets for the COVID-19 Coronavirus (SARS-CoV-2) Based on SARS-
606 CoV Immunological Studies. *Viruses* 12, 254. <https://doi.org/10.3390/v12030254>

607 Chi, X., Yan, R., Zhang, Jun, Zhang, G., Zhang, Y., Hao, M., Zhang, Z., Fan, P., Dong,
608 Y., Yang, Y., Chen, Z., Guo, Y., Zhang, Jinlong, Li, Y., Song, X., Chen, Y., Xia,
609 L., Fu, L., Hou, L., Xu, J., Yu, C., Li, J., Zhou, Q., Chen, W., 2020. A neutralizing
610 human antibody binds to the N-terminal domain of the Spike protein of SARS-
611 CoV-2. *Science*. <https://doi.org/10.1126/science.abc6952>

612 Crawford, K.H.D., Eguia, R., Dingens, A.S., Loes, A.N., Malone, K.D., Wolf, C.R., Chu,
613 H.Y., Tortorici, M.A., Velesler, D., Murphy, M., Pettie, D., King, N.P., Balazs, A.B.,
614 Bloom, J.D., 2020. Protocol and Reagents for Pseudotyping Lentiviral Particles
615 with SARS-CoV-2 Spike Protein for Neutralization Assays. *Viruses* 12, 513.
616 <https://doi.org/10.3390/v12050513>

617 Dong, E., Du, H., Gardner, L., 2020. An interactive web-based dashboard to track
618 COVID-19 in real time. *The Lancet Infectious Diseases* 20, 533–534.
619 [https://doi.org/10.1016/S1473-3099\(20\)30120-1](https://doi.org/10.1016/S1473-3099(20)30120-1)

620 Forni, D., Cagliani, R., Clerici, M., Sironi, M., 2017. Molecular Evolution of Human
621 Coronavirus Genomes. *Trends Microbiol* 25, 35–48.
622 <https://doi.org/10.1016/j.tim.2016.09.001>

623 Gorbalenya, A.E., Baker, S.C., Baric, R.S., de Groot, R.J., Drosten, C., Gulyaeva, A.A.,
624 Haagmans, B.L., Lauber, C., Leontovich, A.M., Neuman, B.W., Penzar, D.,
625 Perlman, S., Poon, L.L.M., Samborskiy, D.V., Sidorov, I.A., Sola, I., Ziebuhr, J.,
626 Coronaviridae Study Group of the International Committee on Taxonomy of
627 Viruses, 2020. The species Severe acute respiratory syndrome-related
628 coronavirus : classifying 2019-nCoV and naming it SARS-CoV-2. *Nature*
629 *Microbiology* 5, 536–544. <https://doi.org/10.1038/s41564-020-0695-z>

630 Gordon, D.E., Jang, G.M., Bouhaddou, M., Xu, J., Obernier, K., White, K.M., O'Meara,
631 M.J., Rezelj, V.V., Guo, J.Z., Swaney, D.L., Tummino, T.A., Huettenhain, R.,
632 Kaake, R.M., Richards, A.L., Tutuncuoglu, B., Fousard, H., Batra, J., Haas, K.,
633 Modak, M., Kim, M., Haas, P., Polacco, B.J., Braberg, H., Fabius, J.M., Eckhardt,
634 M., Soucheray, M., Bennett, M.J., Cakir, M., McGregor, M.J., Li, Q., Meyer, B.,
635 Roesch, F., Vallet, T., Kain, A.M., Miorin, L., Moreno, E., Naing, Z.Z.C., Zhou, Y.,
636 Peng, S., Shi, Y., Zhang, Z., Shen, W., Kirby, I.T., Melnyk, J.E., Chorba, J.S.,
637 Lou, K., Dai, S.A., Barrio-Hernandez, I., Memon, D., Hernandez-Armenta, C.,
638 Lyu, J., Mathy, C.J.P., Perica, T., Pilla, K.B., Ganesan, S.J., Saltzberg, D.J.,
639 Rakesh, R., Liu, X., Rosenthal, S.B., Calviello, L., Venkataramanan, S., Liboy-
640 Lugo, J., Lin, Y., Huang, X.-P., Liu, Y., Wankowicz, S.A., Bohn, M., Safari, M.,
641 Ugur, F.S., Koh, C., Savar, N.S., Tran, Q.D., Shengjuler, D., Fletcher, S.J.,
642 O'Neal, M.C., Cai, Y., Chang, J.C.J., Broadhurst, D.J., Klippsten, S., Sharp, P.P.,
643 Wenzell, N.A., Kuzuoglu, D., Wang, H.-Y., Trenker, R., Young, J.M., Cavero,
644 D.A., Hiatt, J., Roth, T.L., Rathore, U., Subramanian, A., Noack, J., Hubert, M.,
645 Stroud, R.M., Frankel, A.D., Rosenberg, O.S., Verba, K.A., Agard, D.A., Ott, M.,
646 Emerman, M., Jura, N., Zastrow, M. von, Verdin, E., Ashworth, A., Schwartz, O.,
647 d'Enfert, C., Mukherjee, S., Jacobson, M., Malik, H.S., Fujimori, D.G., Ideker, T.,

- 648 Craik, C.S., Floor, S.N., Fraser, J.S., Gross, J.D., Sali, A., Roth, B.L., Ruggero,
649 D., Taunton, J., Kortemme, T., Beltrao, P., Vignuzzi, M., García-Sastre, A.,
650 Shokat, K.M., Shoichet, B.K., Krogan, N.J., 2020. A SARS-CoV-2 protein
651 interaction map reveals targets for drug repurposing. *Nature* 1–13. [https://doi.org/](https://doi.org/10.1038/s41586-020-2286-9)
652 [10.1038/s41586-020-2286-9](https://doi.org/10.1038/s41586-020-2286-9)
- 653 Hoffmann, M., Kleine-Weber, H., Schroeder, S., Krüger, N., Herrler, T., Erichsen, S.,
654 Schiergens, T.S., Herrler, G., Wu, N.-H., Nitsche, A., Müller, M.A., Drosten, C.,
655 Pöhlmann, S., 2020. SARS-CoV-2 Cell Entry Depends on ACE2 and TMPRSS2
656 and Is Blocked by a Clinically Proven Protease Inhibitor. *Cell*.
657 <https://doi.org/10.1016/j.cell.2020.02.052>
- 658 Khailany, R.A., Safdar, M., Ozaslan, M., 2020. Genomic characterization of a novel
659 SARS-CoV-2. *Gene Reports* 19, 100682.
660 <https://doi.org/10.1016/j.genrep.2020.100682>
- 661 Killerby, M.E., Biggs, H.M., Haynes, A., Dahl, R.M., Mustaqim, D., Gerber, S.I.,
662 Watson, J.T., 2018. Human coronavirus circulation in the United States 2014–
663 2017. *Journal of Clinical Virology* 101, 52–56.
664 <https://doi.org/10.1016/j.jcv.2018.01.019>
- 665 Li, F., 2016. Structure, Function, and Evolution of Coronavirus Spike Proteins. *Annu*
666 *Rev Virol* 3, 237–261. <https://doi.org/10.1146/annurev-virology-110615-042301>
- 667 Lv, H., Wu, N.C., Tsang, O.T.-Y., Yuan, M., Perera, R.A.P.M., Leung, W.S., So, R.T.Y.,
668 Chan, J.M.C., Yip, G.K., Chik, T.S.H., Wang, Y., Choi, C.Y.C., Lin, Y., Ng, W.W.,
669 Zhao, J., Poon, L.L.M., Peiris, J.S.M., Wilson, I.A., Mok, C.K.P., 2020. Cross-
670 reactive Antibody Response between SARS-CoV-2 and SARS-CoV Infections.
671 *Cell Reports* 31. <https://doi.org/10.1016/j.celrep.2020.107725>
- 672 Martin, J.E., Louder, M.K., Holman, L.A., Gordon, I.J., Enama, M.E., Larkin, B.D.,
673 Andrews, C.A., Vogel, L., Koup, R.A., Roederer, M., Bailer, R.T., Gomez, P.L.,
674 Nason, M., Mascola, J.R., Nabel, G.J., Graham, B.S., VRC 301 Study Team,
675 2008. A SARS DNA vaccine induces neutralizing antibody and cellular immune
676 responses in healthy adults in a Phase I clinical trial. *Vaccine* 26, 6338–6343.
677 <https://doi.org/10.1016/j.vaccine.2008.09.026>
- 678 McBride, R., Van Zyl, M., Fielding, B.C., 2014. The Coronavirus Nucleocapsid Is a
679 Multifunctional Protein. *Viruses* 6, 2991–3018. <https://doi.org/10.3390/v6082991>
- 680 Neuman, B.W., Kiss, G., Kunding, A.H., Bhella, D., Baksh, M.F., Connelly, S., Droese,
681 B., Klaus, J.P., Makino, S., Sawicki, S.G., Siddell, S.G., Stamou, D.G., Wilson,
682 I.A., Kuhn, P., Buchmeier, M.J., 2011. A structural analysis of M protein in
683 coronavirus assembly and morphology. *Journal of Structural Biology* 174, 11–22.
684 <https://doi.org/10.1016/j.jsb.2010.11.021>
- 685 Schoeman, D., Fielding, B.C., 2019. Coronavirus envelope protein: current knowledge.
686 *Virology Journal* 16, 69. <https://doi.org/10.1186/s12985-019-1182-0>
- 687 Severance, E.G., Bossis, I., Dickerson, F.B., Stallings, C.R., Origoni, A.E., Sullens, A.,
688 Yolken, R.H., Viscidi, R.P., 2008. Development of a Nucleocapsid-Based Human
689 Coronavirus Immunoassay and Estimates of Individuals Exposed to Coronavirus
690 in a U.S. Metropolitan Population. *Clin Vaccine Immunol* 15, 1805–1810.
691 <https://doi.org/10.1128/CVI.00124-08>

- 692 Sullivan, H.C., Roback, J.D., 2020. Convalescent Plasma: Therapeutic Hope or
693 Hopeless Strategy in the SARS-CoV-2 Pandemic. *Transfus Med Rev.*
694 <https://doi.org/10.1016/j.tmr.2020.04.001>
- 695 ter Meulen, J., van den Brink, E.N., Poon, L.L.M., Marissen, W.E., Leung, C.S.W., Cox,
696 F., Cheung, C.Y., Bakker, A.Q., Bogaards, J.A., van Deventer, E., Preiser, W.,
697 Doerr, H.W., Chow, V.T., de Kruif, J., Peiris, J.S.M., Goudsmit, J., 2006. Human
698 Monoclonal Antibody Combination against SARS Coronavirus: Synergy and
699 Coverage of Escape Mutants. *PLoS Med* 3.
700 <https://doi.org/10.1371/journal.pmed.0030237>
- 701 Tian, X., Li, C., Huang, A., Xia, S., Lu, S., Shi, Z., Lu, L., Jiang, S., Yang, Z., Wu, Y.,
702 Ying, T., 2020. Potent binding of 2019 novel coronavirus spike protein by a
703 SARS coronavirus-specific human monoclonal antibody. *Emerg Microbes Infect*
704 9, 382–385. <https://doi.org/10.1080/22221751.2020.1729069>
- 705 Tripp, R.A., Haynes, L.M., Moore, D., Anderson, B., Tamin, A., Harcourt, B.H., Jones,
706 L.P., Yilla, M., Babcock, G.J., Greenough, T., Ambrosino, D.M., Alvarez, R.,
707 Callaway, J., Cavitt, S., Kamrud, K., Alterson, H., Smith, J., Harcourt, J.L., Miao,
708 C., Razdan, R., Comer, J.A., Rollin, P.E., Ksiazek, T.G., Sanchez, A., Rota, P.A.,
709 Bellini, W.J., Anderson, L.J., 2005. Monoclonal antibodies to SARS-associated
710 coronavirus (SARS-CoV): Identification of neutralizing and antibodies reactive to
711 S, N, M and E viral proteins. *Journal of Virological Methods* 128, 21–28.
712 <https://doi.org/10.1016/j.jviromet.2005.03.021>
- 713 Wrapp, D., De Vlieger, D., Corbett, K.S., Torres, G.M., Wang, N., Van Breedam, W.,
714 Roose, K., van Schie, L., Hoffmann, M., Pöhlmann, S., Graham, B.S.,
715 Callewaert, N., Schepens, B., Saelens, X., McLellan, J.S., 2020. Structural Basis
716 for Potent Neutralization of Betacoronaviruses by Single-Domain Camelid
717 Antibodies. *Cell* 181, 1004-1015.e15. <https://doi.org/10.1016/j.cell.2020.04.031>
- 718 Yu, J., Tostanoski, L.H., Peter, L., Mercado, N.B., McMahan, K., Mahrokhian, S.H.,
719 Nkolola, J.P., Liu, J., Li, Z., Chandrashekar, A., Martinez, D.R., Loos, C., Atyeo,
720 C., Fischinger, S., Burke, J.S., Slein, M.D., Chen, Y., Zuiani, A., N. Lelis, F.J.,
721 Travers, M., Habibi, S., Pessaint, L., Van Ry, A., Blade, K., Brown, R., Cook, A.,
722 Finneyfrock, B., Dodson, A., Teow, E., Velasco, J., Zahn, R., Wegmann, F.,
723 Bondzie, E.A., Dagotto, G., Gebre, M.S., He, X., Jacob-Dolan, C., Kirilova, M.,
724 Kordana, N., Lin, Z., Maxfield, L.F., Nampanya, F., Nityanandam, R., Ventura,
725 J.D., Wan, H., Cai, Y., Chen, B., Schmidt, A.G., Wesemann, D.R., Baric, R.S.,
726 Alter, G., Andersen, H., Lewis, M.G., Barouch, D.H., 2020. DNA vaccine
727 protection against SARS-CoV-2 in rhesus macaques. *Science*.
728 <https://doi.org/10.1126/science.abc6284>
- 729 Yuan, M., Wu, N.C., Zhu, X., Lee, C.-C.D., So, R.T.Y., Lv, H., Mok, C.K.P., Wilson, I.A.,
730 2020. A highly conserved cryptic epitope in the receptor binding domains of
731 SARS-CoV-2 and SARS-CoV. *Science* 368, 630–633.
732 <https://doi.org/10.1126/science.abb7269>
- 733 Zhang, L., Pang, R., Xue, X., Bao, J., Ye, S., Dai, Y., Zheng, Y., Fu, Q., Hu, Z., Yi, Y.,
734 2020. Anti-SARS-CoV-2 virus antibody levels in convalescent plasma of six
735 donors who have recovered from COVID-19. *Aging (Albany NY)* 12, 6536–6542.
736 <https://doi.org/10.18632/aging.103102>

- 737 Zhou, P., Yang, X.-L., Wang, X.-G., Hu, B., Zhang, L., Zhang, W., Si, H.-R., Zhu, Y., Li,
738 B., Huang, C.-L., Chen, H.-D., Chen, J., Luo, Y., Guo, H., Jiang, R.-D., Liu, M.-
739 Q., Chen, Y., Shen, X.-R., Wang, X., Zheng, X.-S., Zhao, K., Chen, Q.-J., Deng,
740 F., Liu, L.-L., Yan, B., Zhan, F.-X., Wang, Y.-Y., Xiao, G.-F., Shi, Z.-L., 2020. A
741 pneumonia outbreak associated with a new coronavirus of probable bat origin.
742 *Nature* 579, 270–273. <https://doi.org/10.1038/s41586-020-2012-7>
- 743 Zhu, N., Zhang, D., Wang, W., Li, X., Yang, B., Song, J., Zhao, X., Huang, B., Shi, W.,
744 Lu, R., Niu, P., Zhan, F., Ma, X., Wang, D., Xu, W., Wu, G., Gao, G.F., Tan, W.,
745 2020. A Novel Coronavirus from Patients with Pneumonia in China, 2019. *New*
746 *England Journal of Medicine* 382, 727–733.
747 <https://doi.org/10.1056/NEJMoa2001017>, McKay, M.R., 2020. Preliminary
748 Identification of Potential Vaccine Targets for the COVID-19 Coronavirus (SARS-
749 CoV-2) Based on SARS-CoV Immunological Studies. *Viruses* 12, 254.
750 <https://doi.org/10.3390/v12030254>
- 751 Chi, X., Yan, R., Zhang, Jun, Zhang, G., Zhang, Y., Hao, M., Zhang, Z., Fan, P., Dong,
752 Y., Yang, Y., Chen, Z., Guo, Y., Zhang, Jinlong, Li, Y., Song, X., Chen, Y., Xia,
753 L., Fu, L., Hou, L., Xu, J., Yu, C., Li, J., Zhou, Q., Chen, W., 2020. A neutralizing
754 human antibody binds to the N-terminal domain of the Spike protein of SARS-
755 CoV-2. *Science*. <https://doi.org/10.1126/science.abc6952>
- 756 Crawford, K.H.D., Eguia, R., Dingens, A.S., Loes, A.N., Malone, K.D., Wolf, C.R., Chu,
757 H.Y., Tortorici, M.A., Velesler, D., Murphy, M., Pettie, D., King, N.P., Balazs, A.B.,
758 Bloom, J.D., 2020. Protocol and Reagents for Pseudotyping Lentiviral Particles
759 with SARS-CoV-2 Spike Protein for Neutralization Assays. *Viruses* 12, 513.
760 <https://doi.org/10.3390/v12050513>
- 761 Dong, E., Du, H., Gardner, L., 2020. An interactive web-based dashboard to track
762 COVID-19 in real time. *The Lancet Infectious Diseases* 20, 533–534.
763 [https://doi.org/10.1016/S1473-3099\(20\)30120-1](https://doi.org/10.1016/S1473-3099(20)30120-1)
- 764 Forni, D., Cagliani, R., Clerici, M., Sironi, M., 2017. Molecular Evolution of Human
765 Coronavirus Genomes. *Trends Microbiol* 25, 35–48.
766 <https://doi.org/10.1016/j.tim.2016.09.001>
- 767 Gorbalenya, A.E., Baker, S.C., Baric, R.S., de Groot, R.J., Drosten, C., Gulyaeva, A.A.,
768 Haagmans, B.L., Lauber, C., Leontovich, A.M., Neuman, B.W., Penzar, D.,
769 Perlman, S., Poon, L.L.M., Samborskiy, D.V., Sidorov, I.A., Sola, I., Ziebuhr, J.,
770 Coronaviridae Study Group of the International Committee on Taxonomy of
771 Viruses, 2020. The species Severe acute respiratory syndrome-related
772 coronavirus : classifying 2019-nCoV and naming it SARS-CoV-2. *Nature*
773 *Microbiology* 5, 536–544. <https://doi.org/10.1038/s41564-020-0695-z>
- 774 Gordon, D.E., Jang, G.M., Bouhaddou, M., Xu, J., Obernier, K., White, K.M., O’Meara,
775 M.J., Rezelj, V.V., Guo, J.Z., Swaney, D.L., Tummino, T.A., Huettenhain, R.,
776 Kaake, R.M., Richards, A.L., Tutuncuoglu, B., Foussard, H., Batra, J., Haas, K.,
777 Modak, M., Kim, M., Haas, P., Polacco, B.J., Braberg, H., Fabius, J.M., Eckhardt,
778 M., Soucheray, M., Bennett, M.J., Cakir, M., McGregor, M.J., Li, Q., Meyer, B.,
779 Roesch, F., Vallet, T., Kain, A.M., Miorin, L., Moreno, E., Naing, Z.Z.C., Zhou, Y.,
780 Peng, S., Shi, Y., Zhang, Z., Shen, W., Kirby, I.T., Melnyk, J.E., Chorba, J.S.,
781 Lou, K., Dai, S.A., Barrio-Hernandez, I., Memon, D., Hernandez-Armenta, C.,
782 Lyu, J., Mathy, C.J.P., Perica, T., Pilla, K.B., Ganesan, S.J., Saltzberg, D.J.,

- 783 Rakesh, R., Liu, X., Rosenthal, S.B., Calviello, L., Venkataramanan, S., Liboy-
784 Lugo, J., Lin, Y., Huang, X.-P., Liu, Y., Wankowicz, S.A., Bohn, M., Safari, M.,
785 Ugur, F.S., Koh, C., Savar, N.S., Tran, Q.D., Shengjuler, D., Fletcher, S.J.,
786 O'Neal, M.C., Cai, Y., Chang, J.C.J., Broadhurst, D.J., Klippsten, S., Sharp, P.P.,
787 Wenzell, N.A., Kuzuoglu, D., Wang, H.-Y., Trenker, R., Young, J.M., Cavero,
788 D.A., Hiatt, J., Roth, T.L., Rathore, U., Subramanian, A., Noack, J., Hubert, M.,
789 Stroud, R.M., Frankel, A.D., Rosenberg, O.S., Verba, K.A., Agard, D.A., Ott, M.,
790 Emerman, M., Jura, N., Zastrow, M. von, Verdin, E., Ashworth, A., Schwartz, O.,
791 d'Enfert, C., Mukherjee, S., Jacobson, M., Malik, H.S., Fujimori, D.G., Ideker, T.,
792 Craik, C.S., Floor, S.N., Fraser, J.S., Gross, J.D., Sali, A., Roth, B.L., Ruggero,
793 D., Taunton, J., Kortemme, T., Beltrao, P., Vignuzzi, M., García-Sastre, A.,
794 Shokat, K.M., Shoichet, B.K., Krogan, N.J., 2020. A SARS-CoV-2 protein
795 interaction map reveals targets for drug repurposing. *Nature* 1–13. [https://doi.org/](https://doi.org/10.1038/s41586-020-2286-9)
796 [10.1038/s41586-020-2286-9](https://doi.org/10.1038/s41586-020-2286-9)
- 797 Hoffmann, M., Kleine-Weber, H., Schroeder, S., Krüger, N., Herrler, T., Erichsen, S.,
798 Schiergens, T.S., Herrler, G., Wu, N.-H., Nitsche, A., Müller, M.A., Drosten, C.,
799 Pöhlmann, S., 2020. SARS-CoV-2 Cell Entry Depends on ACE2 and TMPRSS2
800 and Is Blocked by a Clinically Proven Protease Inhibitor. *Cell*.
801 <https://doi.org/10.1016/j.cell.2020.02.052>
- 802 Khailany, R.A., Safdar, M., Ozaslan, M., 2020. Genomic characterization of a novel
803 SARS-CoV-2. *Gene Reports* 19, 100682.
804 <https://doi.org/10.1016/j.genrep.2020.100682>
- 805 Killerby, M.E., Biggs, H.M., Haynes, A., Dahl, R.M., Mustaquim, D., Gerber, S.I.,
806 Watson, J.T., 2018. Human coronavirus circulation in the United States 2014–
807 2017. *Journal of Clinical Virology* 101, 52–56.
808 <https://doi.org/10.1016/j.jcv.2018.01.019>
- 809 Li, F., 2016. Structure, Function, and Evolution of Coronavirus Spike Proteins. *Annu*
810 *Rev Virol* 3, 237–261. <https://doi.org/10.1146/annurev-virology-110615-042301>
- 811 Lv, H., Wu, N.C., Tsang, O.T.-Y., Yuan, M., Perera, R.A.P.M., Leung, W.S., So, R.T.Y.,
812 Chan, J.M.C., Yip, G.K., Chik, T.S.H., Wang, Y., Choi, C.Y.C., Lin, Y., Ng, W.W.,
813 Zhao, J., Poon, L.L.M., Peiris, J.S.M., Wilson, I.A., Mok, C.K.P., 2020. Cross-
814 reactive Antibody Response between SARS-CoV-2 and SARS-CoV Infections.
815 *Cell Reports* 31. <https://doi.org/10.1016/j.celrep.2020.107725>
- 816 Martin, J.E., Louder, M.K., Holman, L.A., Gordon, I.J., Enama, M.E., Larkin, B.D.,
817 Andrews, C.A., Vogel, L., Koup, R.A., Roederer, M., Bailer, R.T., Gomez, P.L.,
818 Nason, M., Mascola, J.R., Nabel, G.J., Graham, B.S., VRC 301 Study Team,
819 2008. A SARS DNA vaccine induces neutralizing antibody and cellular immune
820 responses in healthy adults in a Phase I clinical trial. *Vaccine* 26, 6338–6343.
821 <https://doi.org/10.1016/j.vaccine.2008.09.026>
- 822 McBride, R., Van Zyl, M., Fielding, B.C., 2014. The Coronavirus Nucleocapsid Is a
823 Multifunctional Protein. *Viruses* 6, 2991–3018. <https://doi.org/10.3390/v6082991>
- 824 Neuman, B.W., Kiss, G., Kunding, A.H., Bhella, D., Baksh, M.F., Connelly, S., Droese,
825 B., Klaus, J.P., Makino, S., Sawicki, S.G., Siddell, S.G., Stamou, D.G., Wilson,
826 I.A., Kuhn, P., Buchmeier, M.J., 2011. A structural analysis of M protein in
827 coronavirus assembly and morphology. *Journal of Structural Biology* 174, 11–22.
828 <https://doi.org/10.1016/j.jsb.2010.11.021>

- 829 Schoeman, D., Fielding, B.C., 2019. Coronavirus envelope protein: current knowledge.
830 *Virology Journal* 16, 69. <https://doi.org/10.1186/s12985-019-1182-0>
- 831 Severance, E.G., Bossis, I., Dickerson, F.B., Stallings, C.R., Origoni, A.E., Sullens, A.,
832 Yolken, R.H., Viscidi, R.P., 2008. Development of a Nucleocapsid-Based Human
833 Coronavirus Immunoassay and Estimates of Individuals Exposed to Coronavirus
834 in a U.S. Metropolitan Population. *Clin Vaccine Immunol* 15, 1805–1810.
835 <https://doi.org/10.1128/CVI.00124-08>
- 836 Sullivan, H.C., Roback, J.D., 2020. Convalescent Plasma: Therapeutic Hope or
837 Hopeless Strategy in the SARS-CoV-2 Pandemic. *Transfus Med Rev.*
838 <https://doi.org/10.1016/j.tmr.2020.04.001>
- 839 ter Meulen, J., van den Brink, E.N., Poon, L.L.M., Marissen, W.E., Leung, C.S.W., Cox,
840 F., Cheung, C.Y., Bakker, A.Q., Bogaards, J.A., van Deventer, E., Preiser, W.,
841 Doerr, H.W., Chow, V.T., de Kruif, J., Peiris, J.S.M., Goudsmit, J., 2006. Human
842 Monoclonal Antibody Combination against SARS Coronavirus: Synergy and
843 Coverage of Escape Mutants. *PLoS Med* 3.
844 <https://doi.org/10.1371/journal.pmed.0030237>
- 845 Tian, X., Li, C., Huang, A., Xia, S., Lu, S., Shi, Z., Lu, L., Jiang, S., Yang, Z., Wu, Y.,
846 Ying, T., 2020. Potent binding of 2019 novel coronavirus spike protein by a
847 SARS coronavirus-specific human monoclonal antibody. *Emerg Microbes Infect*
848 9, 382–385. <https://doi.org/10.1080/22221751.2020.1729069>
- 849 Tripp, R.A., Haynes, L.M., Moore, D., Anderson, B., Tamin, A., Harcourt, B.H., Jones,
850 L.P., Yilla, M., Babcock, G.J., Greenough, T., Ambrosino, D.M., Alvarez, R.,
851 Callaway, J., Cavitt, S., Kamrud, K., Alterson, H., Smith, J., Harcourt, J.L., Miao,
852 C., Razdan, R., Comer, J.A., Rollin, P.E., Ksiazek, T.G., Sanchez, A., Rota, P.A.,
853 Bellini, W.J., Anderson, L.J., 2005. Monoclonal antibodies to SARS-associated
854 coronavirus (SARS-CoV): Identification of neutralizing and antibodies reactive to
855 S, N, M and E viral proteins. *Journal of Virological Methods* 128, 21–28.
856 <https://doi.org/10.1016/j.jviromet.2005.03.021>
- 857 Wrapp, D., De Vlieger, D., Corbett, K.S., Torres, G.M., Wang, N., Van Breedam, W.,
858 Roose, K., van Schie, L., Hoffmann, M., Pöhlmann, S., Graham, B.S.,
859 Callewaert, N., Schepens, B., Saelens, X., McLellan, J.S., 2020. Structural Basis
860 for Potent Neutralization of Betacoronaviruses by Single-Domain Camelid
861 Antibodies. *Cell* 181, 1004-1015.e15. <https://doi.org/10.1016/j.cell.2020.04.031>
- 862 Yu, J., Tostanoski, L.H., Peter, L., Mercado, N.B., McMahan, K., Mahrokhian, S.H.,
863 Nkolola, J.P., Liu, J., Li, Z., Chandrashekar, A., Martinez, D.R., Loos, C., Atyeo,
864 C., Fischinger, S., Burke, J.S., Slein, M.D., Chen, Y., Zuiani, A., N. Lelis, F.J.,
865 Travers, M., Habibi, S., Pessaint, L., Van Ry, A., Blade, K., Brown, R., Cook, A.,
866 Finneyfrock, B., Dodson, A., Teow, E., Velasco, J., Zahn, R., Wegmann, F.,
867 Bondzie, E.A., Dagotto, G., Gebre, M.S., He, X., Jacob-Dolan, C., Kirilova, M.,
868 Kordana, N., Lin, Z., Maxfield, L.F., Nampanya, F., Nityanandam, R., Ventura,
869 J.D., Wan, H., Cai, Y., Chen, B., Schmidt, A.G., Wesemann, D.R., Baric, R.S.,
870 Alter, G., Andersen, H., Lewis, M.G., Barouch, D.H., 2020. DNA vaccine
871 protection against SARS-CoV-2 in rhesus macaques. *Science.*
872 <https://doi.org/10.1126/science.abc6284>
- 873 Yuan, M., Wu, N.C., Zhu, X., Lee, C.-C.D., So, R.T.Y., Lv, H., Mok, C.K.P., Wilson, I.A.,
874 2020. A highly conserved cryptic epitope in the receptor binding domains of

- 875 SARS-CoV-2 and SARS-CoV. *Science* 368, 630–633.
876 <https://doi.org/10.1126/science.abb7269>
- 877 Zhang, L., Pang, R., Xue, X., Bao, J., Ye, S., Dai, Y., Zheng, Y., Fu, Q., Hu, Z., Yi, Y.,
878 2020. Anti-SARS-CoV-2 virus antibody levels in convalescent plasma of six
879 donors who have recovered from COVID-19. *Aging (Albany NY)* 12, 6536–6542.
880 <https://doi.org/10.18632/aging.103102>
- 881 Zhou, P., Yang, X.-L., Wang, X.-G., Hu, B., Zhang, L., Zhang, W., Si, H.-R., Zhu, Y., Li,
882 B., Huang, C.-L., Chen, H.-D., Chen, J., Luo, Y., Guo, H., Jiang, R.-D., Liu, M.-
883 Q., Chen, Y., Shen, X.-R., Wang, X., Zheng, X.-S., Zhao, K., Chen, Q.-J., Deng,
884 F., Liu, L.-L., Yan, B., Zhan, F.-X., Wang, Y.-Y., Xiao, G.-F., Shi, Z.-L., 2020. A
885 pneumonia outbreak associated with a new coronavirus of probable bat origin.
886 *Nature* 579, 270–273. <https://doi.org/10.1038/s41586-020-2012-7>
- 887 Zhu, N., Zhang, D., Wang, W., Li, X., Yang, B., Song, J., Zhao, X., Huang, B., Shi, W.,
888 Lu, R., Niu, P., Zhan, F., Ma, X., Wang, D., Xu, W., Wu, G., Gao, G.F., Tan, W.,
889 2020. A Novel Coronavirus from Patients with Pneumonia in China, 2019. *New*
890 *England Journal of Medicine* 382, 727–733.
891 <https://doi.org/10.1056/NEJMoa2001017> Ahmed, S.F., Quadeer, A.A., McKay,
892 M.R., 2020. Preliminary Identification of Potential Vaccine Targets for the
893 COVID-19 Coronavirus (SARS-CoV-2) Based on SARS-CoV Immunological
894 Studies. *Viruses* 12, 254. <https://doi.org/10.3390/v12030254>
- 895 Chi, X., Yan, R., Zhang, Jun, Zhang, G., Zhang, Y., Hao, M., Zhang, Z., Fan, P., Dong,
896 Y., Yang, Y., Chen, Z., Guo, Y., Zhang, Jinlong, Li, Y., Song, X., Chen, Y., Xia,
897 L., Fu, L., Hou, L., Xu, J., Yu, C., Li, J., Zhou, Q., Chen, W., 2020. A neutralizing
898 human antibody binds to the N-terminal domain of the Spike protein of SARS-
899 CoV-2. *Science*. <https://doi.org/10.1126/science.abc6952>
- 900 Crawford, K.H.D., Eguia, R., Dingens, A.S., Loes, A.N., Malone, K.D., Wolf, C.R., Chu,
901 H.Y., Tortorici, M.A., Velesler, D., Murphy, M., Pettie, D., King, N.P., Balazs, A.B.,
902 Bloom, J.D., 2020. Protocol and Reagents for Pseudotyping Lentiviral Particles
903 with SARS-CoV-2 Spike Protein for Neutralization Assays. *Viruses* 12, 513.
904 <https://doi.org/10.3390/v12050513>
- 905 Dong, E., Du, H., Gardner, L., 2020. An interactive web-based dashboard to track
906 COVID-19 in real time. *The Lancet Infectious Diseases* 20, 533–534.
907 [https://doi.org/10.1016/S1473-3099\(20\)30120-1](https://doi.org/10.1016/S1473-3099(20)30120-1)
- 908 Forni, D., Cagliani, R., Clerici, M., Sironi, M., 2017. Molecular Evolution of Human
909 Coronavirus Genomes. *Trends Microbiol* 25, 35–48.
910 <https://doi.org/10.1016/j.tim.2016.09.001>
- 911 Gorbalenya, A.E., Baker, S.C., Baric, R.S., de Groot, R.J., Drosten, C., Gulyaeva, A.A.,
912 Haagmans, B.L., Lauber, C., Leontovich, A.M., Neuman, B.W., Penzar, D.,
913 Perlman, S., Poon, L.L.M., Samborskiy, D.V., Sidorov, I.A., Sola, I., Ziebuhr, J.,
914 Coronaviridae Study Group of the International Committee on Taxonomy of
915 Viruses, 2020. The species Severe acute respiratory syndrome-related
916 coronavirus : classifying 2019-nCoV and naming it SARS-CoV-2. *Nature*
917 *Microbiology* 5, 536–544. <https://doi.org/10.1038/s41564-020-0695-z>
- 918 Gordon, D.E., Jang, G.M., Bouhaddou, M., Xu, J., Obernier, K., White, K.M., O’Meara,
919 M.J., Rezelj, V.V., Guo, J.Z., Swaney, D.L., Tummino, T.A., Huettenhain, R.,
920 Kaake, R.M., Richards, A.L., Tutuncuoglu, B., Fousard, H., Batra, J., Haas, K.,

921 Modak, M., Kim, M., Haas, P., Polacco, B.J., Braberg, H., Fabius, J.M., Eckhardt,
922 M., Soucheray, M., Bennett, M.J., Cakir, M., McGregor, M.J., Li, Q., Meyer, B.,
923 Roesch, F., Vallet, T., Kain, A.M., Miorin, L., Moreno, E., Naing, Z.Z.C., Zhou, Y.,
924 Peng, S., Shi, Y., Zhang, Z., Shen, W., Kirby, I.T., Melnyk, J.E., Chorba, J.S.,
925 Lou, K., Dai, S.A., Barrio-Hernandez, I., Memon, D., Hernandez-Armenta, C.,
926 Lyu, J., Mathy, C.J.P., Perica, T., Pilla, K.B., Ganesan, S.J., Saltzberg, D.J.,
927 Rakesh, R., Liu, X., Rosenthal, S.B., Calviello, L., Venkataramanan, S., Liboy-
928 Lugo, J., Lin, Y., Huang, X.-P., Liu, Y., Wankowicz, S.A., Bohn, M., Safari, M.,
929 Ugur, F.S., Koh, C., Savar, N.S., Tran, Q.D., Shengjuler, D., Fletcher, S.J.,
930 O'Neal, M.C., Cai, Y., Chang, J.C.J., Broadhurst, D.J., Klippsten, S., Sharp, P.P.,
931 Wenzell, N.A., Kuzuoglu, D., Wang, H.-Y., Trenker, R., Young, J.M., Cavero,
932 D.A., Hiatt, J., Roth, T.L., Rathore, U., Subramanian, A., Noack, J., Hubert, M.,
933 Stroud, R.M., Frankel, A.D., Rosenberg, O.S., Verba, K.A., Agard, D.A., Ott, M.,
934 Emerman, M., Jura, N., Zastrow, M. von, Verdin, E., Ashworth, A., Schwartz, O.,
935 d'Enfert, C., Mukherjee, S., Jacobson, M., Malik, H.S., Fujimori, D.G., Ideker, T.,
936 Craik, C.S., Floor, S.N., Fraser, J.S., Gross, J.D., Sali, A., Roth, B.L., Ruggero,
937 D., Taunton, J., Kortemme, T., Beltrao, P., Vignuzzi, M., García-Sastre, A.,
938 Shokat, K.M., Shoichet, B.K., Krogan, N.J., 2020. A SARS-CoV-2 protein
939 interaction map reveals targets for drug repurposing. *Nature* 1–13. [https://doi.org/](https://doi.org/10.1038/s41586-020-2286-9)
940 [10.1038/s41586-020-2286-9](https://doi.org/10.1038/s41586-020-2286-9)

941 Hoffmann, M., Kleine-Weber, H., Schroeder, S., Krüger, N., Herrler, T., Erichsen, S.,
942 Schiergens, T.S., Herrler, G., Wu, N.-H., Nitsche, A., Müller, M.A., Drosten, C.,
943 Pöhlmann, S., 2020. SARS-CoV-2 Cell Entry Depends on ACE2 and TMPRSS2
944 and Is Blocked by a Clinically Proven Protease Inhibitor. *Cell*.
945 <https://doi.org/10.1016/j.cell.2020.02.052>

946 Khailany, R.A., Safdar, M., Ozaslan, M., 2020. Genomic characterization of a novel
947 SARS-CoV-2. *Gene Reports* 19, 100682.
948 <https://doi.org/10.1016/j.genrep.2020.100682>

949 Killerby, M.E., Biggs, H.M., Haynes, A., Dahl, R.M., Mustaquim, D., Gerber, S.I.,
950 Watson, J.T., 2018. Human coronavirus circulation in the United States 2014–
951 2017. *Journal of Clinical Virology* 101, 52–56.
952 <https://doi.org/10.1016/j.jcv.2018.01.019>

953 Li, F., 2016. Structure, Function, and Evolution of Coronavirus Spike Proteins. *Annu*
954 *Rev Virol* 3, 237–261. <https://doi.org/10.1146/annurev-virology-110615-042301>

955 Lv, H., Wu, N.C., Tsang, O.T.-Y., Yuan, M., Perera, R.A.P.M., Leung, W.S., So, R.T.Y.,
956 Chan, J.M.C., Yip, G.K., Chik, T.S.H., Wang, Y., Choi, C.Y.C., Lin, Y., Ng, W.W.,
957 Zhao, J., Poon, L.L.M., Peiris, J.S.M., Wilson, I.A., Mok, C.K.P., 2020. Cross-
958 reactive Antibody Response between SARS-CoV-2 and SARS-CoV Infections.
959 *Cell Reports* 31. <https://doi.org/10.1016/j.celrep.2020.107725>

960 Martin, J.E., Louder, M.K., Holman, L.A., Gordon, I.J., Enama, M.E., Larkin, B.D.,
961 Andrews, C.A., Vogel, L., Koup, R.A., Roederer, M., Bailer, R.T., Gomez, P.L.,
962 Nason, M., Mascola, J.R., Nabel, G.J., Graham, B.S., VRC 301 Study Team,
963 2008. A SARS DNA vaccine induces neutralizing antibody and cellular immune
964 responses in healthy adults in a Phase I clinical trial. *Vaccine* 26, 6338–6343.
965 <https://doi.org/10.1016/j.vaccine.2008.09.026>

- 966 McBride, R., Van Zyl, M., Fielding, B.C., 2014. The Coronavirus Nucleocapsid Is a
967 Multifunctional Protein. *Viruses* 6, 2991–3018. <https://doi.org/10.3390/v6082991>
- 968 Neuman, B.W., Kiss, G., Kunding, A.H., Bhella, D., Baksh, M.F., Connelly, S., Droese,
969 B., Klaus, J.P., Makino, S., Sawicki, S.G., Siddell, S.G., Stamou, D.G., Wilson,
970 I.A., Kuhn, P., Buchmeier, M.J., 2011. A structural analysis of M protein in
971 coronavirus assembly and morphology. *Journal of Structural Biology* 174, 11–22.
972 <https://doi.org/10.1016/j.jsb.2010.11.021>
- 973 Schoeman, D., Fielding, B.C., 2019. Coronavirus envelope protein: current knowledge.
974 *Virology Journal* 16, 69. <https://doi.org/10.1186/s12985-019-1182-0>
- 975 Severance, E.G., Bossis, I., Dickerson, F.B., Stallings, C.R., Orioni, A.E., Sullens, A.,
976 Yolken, R.H., Viscidi, R.P., 2008. Development of a Nucleocapsid-Based Human
977 Coronavirus Immunoassay and Estimates of Individuals Exposed to Coronavirus
978 in a U.S. Metropolitan Population. *Clin Vaccine Immunol* 15, 1805–1810.
979 <https://doi.org/10.1128/CVI.00124-08>
- 980 Sullivan, H.C., Roback, J.D., 2020. Convalescent Plasma: Therapeutic Hope or
981 Hopeless Strategy in the SARS-CoV-2 Pandemic. *Transfus Med Rev.*
982 <https://doi.org/10.1016/j.tmr.2020.04.001>
- 983 ter Meulen, J., van den Brink, E.N., Poon, L.L.M., Marissen, W.E., Leung, C.S.W., Cox,
984 F., Cheung, C.Y., Bakker, A.Q., Bogaards, J.A., van Deventer, E., Preiser, W.,
985 Doerr, H.W., Chow, V.T., de Kruif, J., Peiris, J.S.M., Goudsmit, J., 2006. Human
986 Monoclonal Antibody Combination against SARS Coronavirus: Synergy and
987 Coverage of Escape Mutants. *PLoS Med* 3.
988 <https://doi.org/10.1371/journal.pmed.0030237>
- 989 Tian, X., Li, C., Huang, A., Xia, S., Lu, S., Shi, Z., Lu, L., Jiang, S., Yang, Z., Wu, Y.,
990 Ying, T., 2020. Potent binding of 2019 novel coronavirus spike protein by a
991 SARS coronavirus-specific human monoclonal antibody. *Emerg Microbes Infect*
992 9, 382–385. <https://doi.org/10.1080/22221751.2020.1729069>
- 993 Tripp, R.A., Haynes, L.M., Moore, D., Anderson, B., Tamin, A., Harcourt, B.H., Jones,
994 L.P., Yilla, M., Babcock, G.J., Greenough, T., Ambrosino, D.M., Alvarez, R.,
995 Callaway, J., Cavitt, S., Kamrud, K., Alterson, H., Smith, J., Harcourt, J.L., Miao,
996 C., Razdan, R., Comer, J.A., Rollin, P.E., Ksiazek, T.G., Sanchez, A., Rota, P.A.,
997 Bellini, W.J., Anderson, L.J., 2005. Monoclonal antibodies to SARS-associated
998 coronavirus (SARS-CoV): Identification of neutralizing and antibodies reactive to
999 S, N, M and E viral proteins. *Journal of Virological Methods* 128, 21–28.
1000 <https://doi.org/10.1016/j.jviromet.2005.03.021>
- 1001 Wrapp, D., De Vlieger, D., Corbett, K.S., Torres, G.M., Wang, N., Van Breedam, W.,
1002 Roose, K., van Schie, L., Hoffmann, M., Pöhlmann, S., Graham, B.S.,
1003 Callewaert, N., Schepens, B., Saelens, X., McLellan, J.S., 2020. Structural Basis
1004 for Potent Neutralization of Betacoronaviruses by Single-Domain Camelid
1005 Antibodies. *Cell* 181, 1004–1015.e15. <https://doi.org/10.1016/j.cell.2020.04.031>
- 1006 Yu, J., Tostanoski, L.H., Peter, L., Mercado, N.B., McMahan, K., Mahrokhian, S.H.,
1007 Nkolola, J.P., Liu, J., Li, Z., Chandrashekar, A., Martinez, D.R., Loos, C., Atyeo,
1008 C., Fischinger, S., Burke, J.S., Slein, M.D., Chen, Y., Zuiani, A., N. Lelis, F.J.,
1009 Travers, M., Habibi, S., Pessaint, L., Van Ry, A., Blade, K., Brown, R., Cook, A.,
1010 Finneyfrock, B., Dodson, A., Teow, E., Velasco, J., Zahn, R., Wegmann, F.,
1011 Bondzie, E.A., Dagotto, G., Gebre, M.S., He, X., Jacob-Dolan, C., Kirilova, M.,

1012 Kordana, N., Lin, Z., Maxfield, L.F., Nampanya, F., Nityanandam, R., Ventura,
1013 J.D., Wan, H., Cai, Y., Chen, B., Schmidt, A.G., Wesemann, D.R., Baric, R.S.,
1014 Alter, G., Andersen, H., Lewis, M.G., Barouch, D.H., 2020. DNA vaccine
1015 protection against SARS-CoV-2 in rhesus macaques. *Science*.
1016 <https://doi.org/10.1126/science.abc6284>

1017 Yuan, M., Wu, N.C., Zhu, X., Lee, C.-C.D., So, R.T.Y., Lv, H., Mok, C.K.P., Wilson, I.A.,
1018 2020. A highly conserved cryptic epitope in the receptor binding domains of
1019 SARS-CoV-2 and SARS-CoV. *Science* 368, 630–633.
1020 <https://doi.org/10.1126/science.abb7269>

1021 Zhang, L., Pang, R., Xue, X., Bao, J., Ye, S., Dai, Y., Zheng, Y., Fu, Q., Hu, Z., Yi, Y.,
1022 2020. Anti-SARS-CoV-2 virus antibody levels in convalescent plasma of six
1023 donors who have recovered from COVID-19. *Aging (Albany NY)* 12, 6536–6542.
1024 <https://doi.org/10.18632/aging.103102>

1025 Zhou, P., Yang, X.-L., Wang, X.-G., Hu, B., Zhang, L., Zhang, W., Si, H.-R., Zhu, Y., Li,
1026 B., Huang, C.-L., Chen, H.-D., Chen, J., Luo, Y., Guo, H., Jiang, R.-D., Liu, M.-
1027 Q., Chen, Y., Shen, X.-R., Wang, X., Zheng, X.-S., Zhao, K., Chen, Q.-J., Deng,
1028 F., Liu, L.-L., Yan, B., Zhan, F.-X., Wang, Y.-Y., Xiao, G.-F., Shi, Z.-L., 2020. A
1029 pneumonia outbreak associated with a new coronavirus of probable bat origin.
1030 *Nature* 579, 270–273. <https://doi.org/10.1038/s41586-020-2012-7>

1031 Zhu, N., Zhang, D., Wang, W., Li, X., Yang, B., Song, J., Zhao, X., Huang, B., Shi, W.,
1032 Lu, R., Niu, P., Zhan, F., Ma, X., Wang, D., Xu, W., Wu, G., Gao, G.F., Tan, W.,
1033 2020. A Novel Coronavirus from Patients with Pneumonia in China, 2019. *New*
1034 *England Journal of Medicine* 382, 727–733.
1035 <https://doi.org/10.1056/NEJMoa2001017>

1036
1037
1038
1039
1040
1041
1042
1043
1044
1045
1046
1047
1048
1049
1050
1051
1052
1053
1054
1055
1056